UNIVERSIDADE DE BRASÍLIA UnB
Faculdade de Ceilândia
Programa de Pós-Graduação em Ciências e Tecnologias em Saúde

JUCÉLY MENEGUCCI DOS SANTOS

ELABORAÇÃO DE NANOCOMPÓSITO DE QUITOSANA MAGNÉTICA PARA LIBERAÇÃO CONTROLADA DE 5-HIDROXITRIPTOFANO

CEILANDIA - DF
2014

Universidade de Brasília
Faculdade UnB – Ceilândia
Pós-Graduação em Ciências e Tecnologias em Saúde

JUCÉLY MENEGUCCI DOS SANTOS

ELABORAÇÃO DE NANOCOMPÓSITO DE QUITOSANA MAGNÉTICA PARA LIBERAÇÃO CONTROLADA DE 5-HIDROXITRIPTOFANO

Dissertação apresentada como requisito para a obtenção do Título de mestre em Ciências e Tecnologias em Saúde pelo programa de Pós-Graduação em Ciências e Tecnologias em Saúde da Universidade de Brasília – Faculdade UnB – Ceilândia.

Orientador: Profº. Dr. Marcelo Henrique Sousa

CEILANDIA - DF
2014

ELABORAÇÃO DE NANOCOMPÓSITO DE QUITOSANA MAGNÉTICA PARA LIBERAÇÃO CONTROLADA DE 5-HIDROXITRIPTOFANO

JUCÉLY MENEGUCCI DOS SANTOS

Dissertação Aprovada em:_____/_____/_____.

Banca Examinadora:

_____

Orientador - Profº Dr. Marcelo Henrique Sousa

_____

1º Membro – Dr. Alexandre Luis Parize

_____

2º Membro – Drª Maria Hosana Conceição

CEILANDIA-DF

2014

DEDICATÓRIA

À minha família, em especial a minha filha Sophia; por compreender ou ao menos tentar entender minha ausência durante este período. Dedico a todos os amigos de laboratório que de algum modo me incentivaram e participaram na construção efetiva desta dissertação. Ao meu orientador pelo incentivo e constante busca do saber.

RESUMO

A elaboração e o refinamento de sistemas de liberação controlada têm sido extensivamente estudados a fim de se aprimorar as terapias com fármacos convencionais e aumentar a adesão do paciente ao tratamento. Para esses fins, vários polímeros biodegradáveis – como a quitosana – conjugados com outros materiais que trazem respostas estímulo-responsíveis ao compósito – como magnetismo – têm sido usados na pesquisa de transporte e liberação de fármacos. Nesse tipo de formulação, o comportamento físico-químico do biopolímero permite a incorporação do princípio ativo na sua estrutura e as estruturas magnéticas agem como sondas para conduzir magneticamente o compósito a uma região específica e/ou, por meio de suas propriedades físicas, causar uma hipertermia magnética que pode controlar a liberação de determinado fármaco pela aplicação de um campo magnético externo. Assim, nesse trabalho, nanoestruturas de quitosana de ~100 nm, incrustradas com até 25% de nanopartículas magnéticas de óxidos de ferro (magnetita/maguemita) de ~5 nm foram produzidas por precipitação em meio homogêneo, pela decomposição da ureia. Nessa mesma, e única etapa de síntese, o 5-hidroxitriptofano foi incorporado ao compósito, com uma eficiência de até 80 %. A caracterização química, morfológica e estrutural foi feita por XRD, TEM, FTIR, TGA, medidas de magnetização e de potencial zeta, enquanto a eficiência de incorporação e o perfil de liberação foram estudados por UV-vis. A cinética de liberação mostrou que trata-se de um sistema de liberação controlada pH-sensitivo governada pelo entumescimento e/ou dissolução da fase polimérica, sendo mais efetiva em meio ácido. O difratograma revela que há coexistência entre a fase polimérica e a magnética; por outro lado a espectroscopia no infravermelho confirma a interação entre quitosana e magnetita. O nanocompósito apresentou uma magnetização de saturação de 11 emu/g enquanto que a do material magnético foi de 50 emu/g; comparável à das ferritas; em função da análise termogravimétrica o nanocompósito apresentou um percentual de 24,6% de nanopartículas magnéticas.

Palavras-chave: liberação controlada, quitosana, nanopartículas magnéticas, L-5-hidroxitriptofan

ABSTRACT

Design and tailoring of controlled release systems have been extensively studied in order to enhance drug therapy and increase patient compliance. For these purposes, various biodegradable polymers – such as chitosan – conjugated with another material which brings stimuli-responsive features – such as magnetism – to the composite have been used in drug delivery research. In this formulation, the physical-chemical behavior of biopolymer allows incorporation of pharmaceuticals in its structure and opens the possibility for applications in drug delivery. Here, the nanomagnets act as probes to magnetically drive the composite to a specific region and/or, through their magneto-thermal properties, can control a drug release with an external magnetic field. Thus, in this work, ~100 nm sized nanoparticles of chitosan embedded with 25 % (w/w) of iron oxide magnetic nanoparticles (magnetite/maghemite) and with a loading efficiency of about 80% for 5-hydroxytryptophan were synthesized, using homogeneous precipitation by urea decomposition, in an efficient one-step procedure. Characterization of morphology, structure and surface were performed by XRD, TEM, FTIR, TGA, magnetization and zeta potential measurements, while drug loading and drug releasing were investigated using UV-vis spectroscopy. Kinetic drug release experiments under different pH conditions revealed a pH-sensitive controlled-release system, ruled by polymer swelling and/or particle dissolution, and that drug release is more efficient in an acidic medium. he XRD pattern reveals that there is coexistence between the polymer phase and magnetic; On the other hand the infrared spectroscopy confirms the interaction between chitosan and magnetite. The nanocomposite showed a saturation magnetization of 11 emu / g while that of the magnetic material was 50 emu / g; comparable to ferrites; depending on the thermal analysis the nanocomposite showed a percentage of 24.6% of magnetic nanoparticles.

Keywords: controlled release, chitosan, magnetic nanoparticles, L-5-Hydroxitriptophan

LISTA DE FIGURAS

LISTA DE ABREVIATURAS E SIGLAS

CS: Quitosana

FTIR: Espectroscopia de transmissão no infra vermelho

JMMM: Journal of Magnetism and Magnetic Materials

MCE: Mínima concentração efetiva

MCT: Mínima concentração tóxica

MHT: Magneto hipertemia

MET: Microscopia eletrônica de Transmissão

UV – *vis*: Espectroscopia de absorção molecular no ultra violeta e visível

XRD: Difração de raio X

SUMÁRIO

CAPÍTULO 1

Introdução geral e Objetivos do trabalho

1. APRESENTAÇÃO

Esse trabalho de dissertação de mestrado foi elaborado na modalidade de artigo científico, conforme previsto nas normas de preparo de trabalhos para obtenção do título de mestre, do Programa de Pós-Graduação em Ciências e Tecnologias em Saúde. Dessa maneira, é composto por uma introdução geral (Capítulo 1), na qual se faz uma apresentação da estrutura do trabalho e do tema de pesquisa, além de sua contextualização e contribuição à literatura científica, ao ensejo, ainda são apresentadas as objetivos do trabalho.

No segundo capítulo é apresentado um artigo científico, cujo principal autor é atual mestranda, intitulado "***One-step synthesis of magnetic chitosan for controlled release of tryptophan***", no qual se resumem a maioria dos resultados obtidos durante este trabalho de mestrado. Foi publicado no periódico *Journal of Magnetism and Magnetic Materials (JMMM),* um dos mais importantes na área de nanomateriais magnéticos aplicados à saúde, que tem um fator de impacto igual a 1,83 e é classificado como A2 no QUALIS da Capes, na área interdisciplinar (avaliado em junho de 2014).

No capítulo 3 é apresentada uma discussão geral sobre o trabalho e são listadas as conclusões e as perspectivas em relação aos resultados obtidos. Em seguida são listadas as referências bibliográficas, principais e suplementares, não envolvidas na elaboração dos artigos científicos. Finalmente, nos anexos, há um documento contendo as normas específicas do periódico JMMM, ao qual o artigo do capítulo 2 foi submetido é contido. Relevante também a inserção, no Anexo C do artigo "***Fabrication of glycine-functionalized maghemite nanoparticles for magnetic removal of copper from wastewater***", publicado como trabalho secundário durante o mestrado, no periódico *Journal of Hazardous Materials*, que tem um fator de impacto igual a 4,68 e é classificado como A1 no QUALIS da Capes, na área interdisciplinar (avaliado em junho de 2014).

2. INTRODUÇÃO

A elaboração e o refinamento de sistemas de liberação controlada têm sido extensivamente estudados, a fim de se aprimorar as terapias com fármacos convencionais e aumentar a adesão do paciente ao tratamento. Isso se tornou possível, uma vez que esses sistemas de liberação controlada podem modular a

exposição de um fármaco em função do tempo, auxiliar o transporte de princípios ativos através das barreiras fisiológicas, proteger medicamentos e fármacos de uma eliminação precoce, conduzir fármacos a um sítio específico, minimizar a exposição e reduzir a frequência de administração de medicamentos (Tran et al., 2011). Para esses propósitos, vários polímeros biodegradáveis têm sido utilizados. Eles podem efetivamente transportar a droga para um sítio-alvo específico e, assim, aumentar o seu benefício terapêutico, minimizando os efeitos adversos (Soppimath et al., 2001).

Um dos biopolímeros que tem atraído a atenção no campo da liberação controlada é a quitosana (CS), um polissacarídeo natural que apresenta baixa toxicidade, propriedade mucoadesiva elevada e características antimicrobianas. Além disso, é pouco alergênico e facilmente removido do organismo. Do ponto de vista químico, a CS apresenta grupamentos amina (NH_2) e hidroxilas (OH) disponíveis para interação com fármacos e outras biomoléculas. Apesar de todas essas vantagens, a CS apresenta algumas restrições físicas que limitam suas propriedades de adsorção – baixa resistência mecânica, baixa estabilidade em meio ácido, baixa densidade e alta taxa de entumescimento (Agnihotri et al., 2004).

Entretanto, essas restrições podem ser minimizadas se o biopolímero for conjugado com outro material que oferece características estímulo-responsíveis ao compósito. Nesse contexto, a CS pode ser conjugada com materiais magnéticos que são extremamente úteis para o desenvolvimento de sistemas de carreamento e de liberação controlada de fármacos inteligentes – a presença de materiais magnéticos permite detectabilidade por técnicas de imagem e diagnóstico, manipulabilidade externa por um campo magnético aplicado e aquecimento pela aplicação de um campo magnético alternado, que pode ser usado para controle da liberação do fármaco (You et al., 2010; Reddy et al 2012).

As nanopartículas magnéticas também são amplamente utilizadas em aplicações biomédicas, uma vez que apresentam grande relação área/volume (*i.e.* área superficial disponível), facilidade para conjugar biomoléculas e manipulabilidade externa por campos magnéticos. Também apresentam baixa taxa de sedimentação e grande penetrabilidade nos tecidos (Pankhurst et al., 2009).

Entretanto, devido a sua natureza química – normalmente são óxidos metálicos ou metais – não são biocompatíveis e necessitam ser funcionalizadas

antes de serem aplicadas no meio biológico. Isso pode ser conseguido pela encapsulação ou dispersão das nanopartículas magnéticas em uma matriz polimérica biocompatível (Reddy et al., 2012). Assim, a combinação das nanopartículas magnéticas com a quitosana poderia incrementar as características dos dois materiais para novas aplicações. É nessa direção que existem relatos da elaboração de quitosana conjugada com materiais magnéticos para diferentes propósitos que vão de aplicações como adsorventes de contaminantes na área ambiental (Reddy, Lee; 2013), para o transporte e liberação de fármacos (Anirudhan et al., 2014) e para magneto hipertermia, na área biomédica (Bae et al., 2012).

Apesar da potencialidade descrita, nanocompósito magnético como veículo de fármacos para liberação controlada não têm sido amplamente exploradas. Além disso, procedimentos simples e reprodutíveis para elaborar sistemas de liberação controlada inteligentes, com propriedades magneto-responsíveis, que possam proporcionar eficiente incorporação do fármaco, liberação modulada e controlada e capacidade de imageamento, são amplamente desejáveis. Nesse sentido, esse trabalho propõe um procedimento simples para a elaboração de um nanocompósito que consiste em nanopartículas de quitosana incrustadas de nanopartículas magnéticas, como um sistema magneto-responsivo para liberação de fármacos. A principal novidade e ineditismo desse trabalho estão situados na rota de síntese proposta, que é ambientalmente correta e compreende a obtenção do compósito e a incorporação do fármaco em única etapa. Neste trabalho, o triptofano foi escolhido como substância ativa, principalmente pela sua grande afinidade com a quitosana e os óxidos de ferro e por ser facilmente monitorado por espectroscopia de absorção molecular no ultravioleta e visível, apesar de apresentar características farmacêuticas bastante apreciáveis e interessantes (Majumdar; 1982). Do ponto de vista farmacológico; o 5-hidroxitriptofano está envolvido na síntese se serotonina uma vez que a concentração serotonina é liberada; observa-se uma elevação do humor do indivíduo; bem como o aumento da capacidade cognitiva; desta maneira sua importância se revela em função de possível desenvolvimento de fármacos tanto para tratamento de depressão; quanto de Alzheimer (Blush, Hazelwood; 2012)

Assim, foi feita a síntese, por meio de precipitação em meio homogêneo, de nanocompósitos de partículas de quitosana, de aproximadamente 100 nm, com 25 % em massa de nanopartículas magnéticas de óxido de ferro embutidas

(magnetita/maguemita). A eficiência de incorporação de 5-hidroxitriptofano foi de até 80 % em um procedimento simplificado, feito em uma única etapa, juntamente com a síntese dos nanomateriais. A caracterização da morfologia, estrutura e superfície foi feita por difração de raios X, microscopia eletrônica de transmissão de alta resolução, espectroscopia de infravermelho, análise termogravimétrica, medidas de magnetização e do potencial zeta. A incorporação e os estudos de liberação do fármaco foram feitos por espectroscopia de absorção no ultravioleta-visível. Estudos da cinética de liberação do 5-hidroxitriptofano em diferentes pHs mostraram que o sistema investigado tem a liberação sensível ao pH do meio e que esse processo de liberação do fármaco é guiado pelo entumescimento e decomposição do polímero.

2.1 Contextualização e contribuição do estudo à literatura científica

2.1.1 Sistemas de liberação controlada e nanomateriais

Sistemas de liberação controlada têm sido desenvolvidos para aperfeiçoar a disponibilidade espacial e temporal de fármacos e outros compostos (genericamente referidos como “fármacos” nesse trabalho) no organismo, principalmente com a finalidade de proteger a droga de degradação ou eliminação fisiológica. Uma terapia não tóxica e eficaz requer que a concentração da droga no plasma esteja dentro de uma janela terapêutica, cujos limites inferior e superior são, respectivamente, a mínima concentração efetiva (MCE) e a mínima concentração tóxica (MCT). Para fármacos rapidamente adsorvidas/eliminadas, uma dose única, indicada pela seta vermelha na figura 1, leva a um aumento rápido e queda rápida na concentração dessa droga (curva com linha sólida no gráfico). Múltiplas doses em intervalos regulares (setas azuis) levam a uma oscilação na concentração da droga que pode ficar fora da janela terapêutica por significantes períodos de tempo, conforme mostrado na curva de pontos da figura 1. Entretanto, se administrado em dose correta, no caso de um sistema de liberação controlada, conforme representada pela curva de traços e pontos, após um rápido aumento, a concentração da droga pode se manter constante, entre os limites da mínima concentração efetiva e da mínima concentração tóxica (Siegel, Rathbone; 2012).

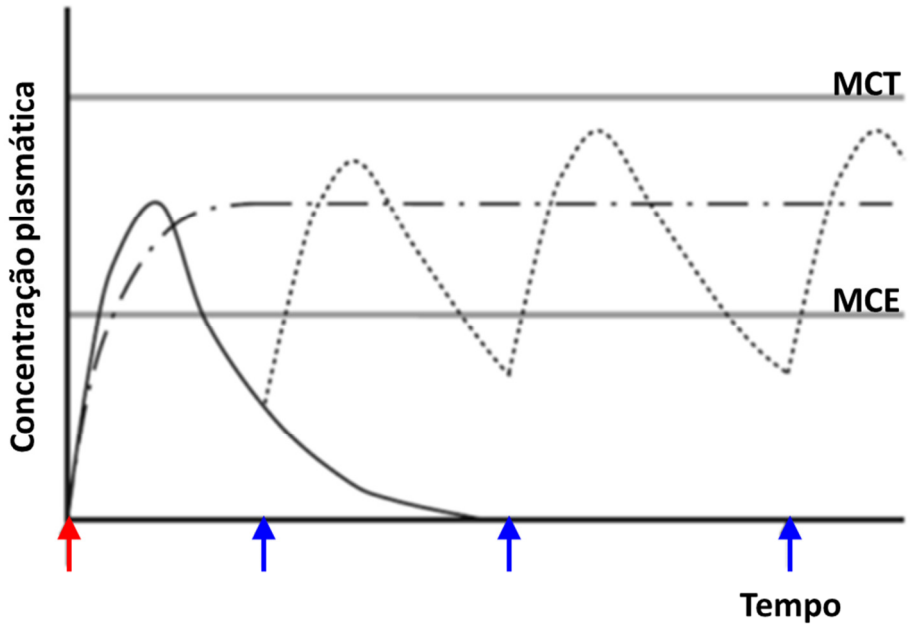

Figura 1. Curvas de janela terapêutica contendo a mínima concentração efetiva (MCE) e a mínima concentração tóxica (MCT)
Fonte: Siegel, Rathbone; 2012

Uma das metodologias mais eficazes para construção de sistemas de liberação controlada é a utilização de nanomateriais. De acordo com Azevedo 2002; os mesmos envolvem estruturas diferentes, como a nanoesfera e a nanocápsula. A nanoesfera é um sistema em que o ativo encontra-se disperso homogeneamente no interior da matriz polimérica, consistindo de um sistema monolítico em que não é possível a identificação de um núcleo, por outro lado na nanocápsula, o fármaco é envolvido por uma membrana que o separa do meio externo, sendo um sistema reservatório onde existe a possibilidade de identificar um núcleo diferenciado. De fato, a grande relação entre a área superficial e volume, além da possibilidade de se obter nanomateriais de composições múltiplas e com propriedades físicas e físico-químicas as mais variadas possíveis, permite ampla interação entre fármaco e nanoestrutura, tornando esses materiais veículos com usos e aplicações infinitas na área de liberação de fármacos. Dessa forma, o emprego de nanopartículas para transporte ou liberação de fármacos conduz a uma maior absorção de um dado fármaco, e em especial no local ou sítio específico que se pretende reduzindo, de maneira considerável, efeitos adversos (Uria; et al., 2007). No entanto, quando se requer sistemas de liberação de medicamentos, seja prolongada ou retardada, deve-

se primeiramente questionar a modulação da resposta pretendida frente ao tipo de liberação desejada (Pezzini, 2007; Coelho et al., 2010).

É nessa direção que existem diversos tipos de sistemas para liberação controlada envolvendo nanotecnologia. As vertentes mais comuns de aplicação são na forma de nanopartículas maciças, nas quais o ativo encontra-se disperso homogeneamente no interior da matriz nanométrica e de nanocápsulas, em que o fármaco é envolvido por uma membrana que o separa do meio externo (Azevedo 2002; Schaffazick et al., 2004). Além disso, ainda existem outras formas de veiculação como aquelas baseadas em emulsões, nanogéis e lipossomas (De Jong et al., 2008).

As matrizes nanométricas são as mais variadas possíveis e vão desde inorgânicas, como sílica e alguns óxidos, até orgânicas e biológicas, como polímeros e proteínas. Para aplicações em liberação controlada, as matrizes poliméricas, e em especial as biodegradáveis, são as mais utilizadas, uma vez que apresentam grande biocompatibilidade e afinidade com fármacos, além de poderem ser estimuladas externamente por parâmetros como pH, temperatura, radiação térmica e eletromagnética, para modular a taxa de liberação das substâncias ativas (Soppimath et al., 2001).

Nessa direção, especial atenção é dada a polímeros naturais, que sofrem biodegradação *in vivo* por ação de enzimas ou micro-organismos. Com grande vantagem, os polissacarídeos são objeto de intenso estudo no sistema de liberação de fármacos, destacando-se a quitosana (CS). Esse polímero apresenta um custo mais baixo em relação aos sintéticos, é biocompatível com os sistemas biológicos e possui grande afinidade com diferentes princípios ativos (Severino et al., 2011; Villanova et al., 2010)**.**

2.1.2 Quitosana

A CS, polisacarídeo com estrutura similar à celulose, conforme mostrado na figura 2, é obtida a partir da desacetilação da quitina, muito comum na fibra ou no exoesqueleto das carapaças dos crustáceos. Sua pureza está relacionada ao nível de desacetilação – entre 50 e 95 % – e seu peso molecular pode atingir até 20 Kg/mol. As aminas primárias conferem à CS propriedades muito apreciadas em aplicações farmacêuticas já que, comparada a outros polímeros, apresenta carga

positiva e é mucoadesiva. Esses grupos amina apresentam-se desprotonados, fazendo com que a CS seja insolúvel em pHs neutros e básicos. À medida que o meio se torna ácido, a CS se torna solúvel em água, uma vez que os grupos amina tendem a se protonar. A solubilidade da CS, entretanto, depende também do grau de desacetilação da amostra. Em geral, soluções de CS são preparadas em soluções diluídas de ácido acético (Madihalie, Mattew; 1999).

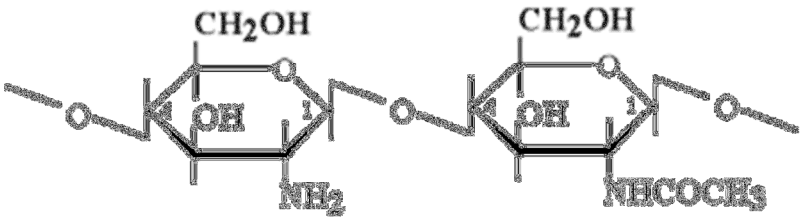

Figura 2. Estrutura molecular da Quitosana
Fonte: Madihalie, Mattew; 1999

Em função de sua propriedade mucoadesiva; pode-se relaciona-la à capacidade que a mesma possui em promover um direcionamento mais específico do fármaco e uma retenção e proteção melhorada do mesmo (Carvalho, Chorilli, Gremião; 2014)

A CS, que apresenta grande biocompatibilidade, é pouco alergênica e raramente é rejeitada pelo organismo, é degradada a produtos ainda menos tóxicos, que são completamente adsorvidos pelo corpo humano. Na área biotecnológica é bastante utilizada como adsorvente para contaminantes do meio ambiente e, na área médica, como suporte sólido para carreamento e liberação controlada de fármacos. De fato, a CS apresenta grande vantagem nessas áreas já que os seus grupos funcionais mimetizam grupos presentes em biomoléculas e fármacos, aumentando a interação entre essas espécies e, além disso, pode ser sintetizada por vias verdes, sem a utilização de solventes ou reagentes agressivos ou nocivos aos organismos em que são aplicadas. Dessa maneira, tendo em vista as diversas características e vantagens relacionadas, existem diversos relatos da elaboração e aplicação de CS, em escala micrométrica e nanométrica, na liberação controlada de fármacos (Brugnerotto et al., 2001 ; Agnihotri; et al. ; 2004).

Uma nova vertente, ligada à produção de biomateriais que respondam ao seu ambiente, tem sido amplamente pesquisada nessa área de liberação controlada de

fármacos. Esses novos materiais, normalmente designados como “materiais inteligentes” ou “estímulo-responsíveis” são capazes de carrear determinado agente terapêutico e, com base em estímulos externos ou variações no ambiente, modular a taxa de liberação dessas substâncias com maior precisão. Polímeros que respondem a diferentes estímulos, tais como pH, temperatura, radiação, ultrassom e magnetismo têm sido amplamente investigados nessa direção, e a CS é um desses materiais. Entretanto, apesar de ser sensível a mudanças ambientais como temperatura e pH, a CS não pode ser facilmente estimulada remotamente. É nesse sentido que materiais multicomponentes e compósitos têm sido fabricados: a combinação de múltiplas possibilidades de estímulos diferenciados permite a utilização de materiais inicialmente inviáveis e potencializa, ainda mais, as possibilidades de aplicação de materiais comumente utilizados. O uso de materiais magnéticos combinados com polímeros biodegradáveis é um desses exemplos. De fato, esses materiais apresentam três principais vantagens: (i) podem ser facilmente localizados por técnicas de diagnóstico no organismo em que são veiculados; (ii) podem ser externamente manipulados e direcionados dentro do organismo por meio da aplicação de campos magnéticos; (iii) podem ser aquecidos pela aplicação de campos magnéticos alternados, facilitando a liberação de princípios ativos ou morte celular por termólise (You et al., 2010).

2.1.3 Nanomateriais magnéticos

O emprego de nanoestruturas em técnicas de diagnósticos e tratamentos tem aumentado potencialmente nos últimos anos (Shi et al., 2010). Mais especificamente, nas últimas décadas, essas investigações têm sido direcionadas para utilização de materiais nanoestruturados que também apresentam *propriedades magnéticas* (Pankhurst et al., 2013). A versatilidade de tais materiais como ferramenta nessa área surge, principalmente, devido a alguns fatores: uma vez que as nanopartículas possuem dimensões menores ou comparáveis à de uma célula, um vírus, uma proteína ou mesmo de um gene, as mesmas podem, facilmente, interagir com uma entidade biológica de interesse, além de permear pelos compartimentos diferenciados do organismo; essas nanopartículas magnéticas podem ser recobertas, ou seja, funcionalizadas por moléculas bioativas, por exemplo, moléculas orgânicas, polímeros, anticorpos, etc, isto é, materiais facilmente reconhecidos por células, tecidos e órgãos do corpo humano, otimizando

sua interação com o organismo, ou mesmo tornando-as pontualmente específicas a uma determinada região ou alvo; uma vez que são magnéticas, as nanopartículas podem ser facilmente manipuladas por gradiente de campo magnético externo e, essa "ação à distância", combinada com a intrínseca penetrabilidade dos campos magnéticos em tecidos humanos, oferece muitas aplicações envolvendo o transporte e/ou imobilização dessas entidades biológicas magneticamente caracterizadas. Desse modo, as nanoestruturas podem ser guiadas ou localizadas em um alvo específico por campos magnéticos externos, tornando-as potenciais carreadoras de fármacos com especificidade de sítio (Berry, 2003; Gupta, 2005; Dobson, 2006; Laurent, 2008; Zhang, 2008), suprindo a não especificidade dos sistemas de veiculação não-magnéticos convencionais. A possibilidade de que as fármacos sejam guiadas e retidas em uma região específica do corpo permite que doses menores sejam administradas, reduzindo os efeitos adversos associados à sobrecarga do organismo por altas doses de medicamento. O potencial de aplicação biomédica desses sistemas, todavia, ultrapassa esse uso e podem ser utilizados também em outras aplicações tanto *in vivo* como *in vitro*. As aplicações *in vivo* compreendem as aplicações terapêuticas (carreamento de fármacos e magnetohipertermia) e diagnósticas (agentes de contraste em imagens de ressonância magnética nuclear Neuberger T et al., 2005), ao passo que as *in vitro* compreendem aquelas diagnósticas (separação magnética de células ou moléculas biológicas variadas e seleção celular). Particularmente promissor, o processo de magnetohipertermia envolve a introdução de nanopartículas magnéticas em um tecido doente e a aplicação de um campo magnético alternado, de intensidade e frequência adequados, suficiente para causar um aquecimento das nanoestruturas. Este aquecimento é imediatamente transmitido ao tecido em questão, de tal forma que, se a temperatura puder ser mantida acima dos 42ºC por tempo adequado, o tecido é normalmente destruído. Além disso, a MHT pode otimizar os processos de liberação controlada de fármacos conjugados a sistemas MNP-polímero, já que o aquecimento desse compósito induz uma "degradação" ou abrandamento do polímero e permite o controle da liberação do fármaco. As investigações da aplicação de materiais magnéticos para hipertermia datam desde os anos 50 e mostram uma grande variedade de aparatos para a aplicação de campos magnéticos de intensidades e frequências diferentes.

Historicamente, para aplicações biomédicas, os óxidos de ferro (Fe_3O_4 e γ-Fe_2O_3) são de longe os nanomateriais mais comumente utilizados como, por exemplo, como contrastantes em ressonância magnética nuclear (Kopp AF; 1997) e como nanocarreadores em hipertermia (Johannsen M.; 2010) clínica. De fato, materiais com valores de magnetização maiores, como cobalto, níquel e ferro metálicos são tóxicos, susceptíveis à oxidação e, portanto, pouco interessantes. Não obstante, em escala nanométrica, esses óxidos magnéticos apresentam fenômenos remarcáveis, destacando-se o superparamagnetismo, as irreversibilidades em campo elevado, altos campos de saturação de magnetização, contribuições extra de anisotropia, fenômenos de superfície, etc., muito apreciados para seu uso em magnetohipertermia. Também o comportamento magnético dessas partículas, acima de certa temperatura (temperatura de bloqueio), é idêntico ao dos átomos paramagnéticos (superparamagnetismo), exceto pelo alto valor de momento magnético dos nanograos (~10^4 magnétons de Bohr). Particularmente, as aplicações biomédicas exigem nanopartículas estáveis e dispersas em meio aquoso neutro e de salinidade fisiológica. A estabilidade coloidal desses sóis depende, nesse caso, primeiramente das dimensões das partículas, que devem ser suficientemente pequenas, evitando sedimentação por ação gravitacional e, também, de sua carga e de sua superfície química, que dão origem a ambas, repulsões estéricas e coulômbicas. As restrições adicionais para aplicação destas nanopartículas estão vinculadas à afinidade das mesmas ao meio biológico. Neste sentido, as partículas devem ser funcionalizadas, *i.e.* recobertas por materiais biocompatíveis, durante ou após o processo de síntese, para evitar a formação de agregados, mudanças da estrutura e composição originais e biodegradação, quando expostas ao meio biológico. Essa superfície funcionalizada também pode permitir o acoplamento de outras biomoléculas, que aumentam sua especificidade, por meio de interações iônicas ou moleculares (Babes L.; 1999).

A síntese de nanopartículas de óxidos de ferro para várias aplicações biomédicas, incluindo a estabilização coloidal com modificações superficiais adequadas e caracterizações físico-químicas estão sumarizadas em alguns artigos de revisão (Roca AG; 2009). Nesses trabalhos, as principais estratégias para obtenção dos núcleos de óxido magnético podem ser classificadas em síntese em meio aquoso, síntese em fase orgânica e síntese por processos de microemulsão. Cada tipo de processo apresenta vantagens e desvantagens para aplicações

biomédicas. Enquanto a síntese em meio aquoso é mais limitada quanto ao controle da morfologia e distribuição em tamanho, esse método produz nanopartículas mais facilmente funcionalizáveis e com menor toxicidade e maior afinidade com o meio biológico. Os métodos orgânicos permitem maior controle de morfologia e, principalmente, de polidispersão. Entretanto, os produtos, ao final da síntese, carregam compostos e solventes orgânicos, dificultando posterior funcionalização e limitando a aplicação em meio biológico, devido ao alto grau de toxicidade. Já as técnicas de microemulsão produzem nanomateriais mais brandos que os processos orgânicos, com um bom controle de tamanho, porém em pequenas quantidades. Além disso, esses trabalhos, conforme já mencionado, se limitam à produção de magnetita e maguemita. Outros óxidos similares, as ferritas espinélio MFe_2O_4 (M = Co^{2+}, Mn^{2+}, Ni^{2+}, Cu^{2+} e Zn^{2+}) também apresentam propriedades magnéticas muito interessantes e, se devidamente funcionalizadas, podem ser usadas, com vantagem, em MHT (Verde, EL. et al., 2012; Verde, EL et al. 2012).

A carga e o caráter hidrofóbico/hidrofílico da superfície têm influência significativa na distribuição *in vivo* das nanopartículas em cada tecido e compartimento microscópico do organismo e na associação das mesmas com biomoléculas do fluido biológico. Em geral, na biocompatibilização das nanopartículas, o material usado para realizar a cobertura deve recobrir suficientemente a superfície do óxido para prevenir interações dos metais superficiais com o meio biológico e permitir a introdução de grupos funcionais e espaçadores para a conjugação com moléculas bioativas, incluindo proteínas, anticorpos, lecitinas, peptídeos, hormônios, vitaminas, nucleotídeos ou fármacos. Além disso, na MHT, essa cobertura deve ser boa transmissora de calor ou, na liberação de fármacos assistida por MHT, ter características termoplásticas adequadas. Em geral, os óxidos magnéticos são encapsulados por compostos poliméricos orgânicos (Ziolo RF; 1992) como quitosana ou por matrizes inorgânicas como a sílica (del Monte F; 1997). Este processo permite modificar a superfície das partículas, com materiais de química já bastante conhecida e estudada, de tal maneira que as partículas podem ter grupamentos químicos específicos que facilitem a ligação da biomolécula de interesse. Os processos de encapsulação tradicionais, porém, aumentam muito o volume das nanopartículas e, por portarem materiais “não-magnéticos”, os nanograos encapsulados apresentam magnetização menos intensa. Estes efeitos são indesejáveis, já que podem limitar suas aplicações

biomédicas, especialmente em MHT. Uma alternativa para contornar esses problemas é a utilização de polímeros biocompatíveis que podem ser depositados, de maneira mais controlada, na superfície dos nanograos magnéticos, como a quitosana.

De fato, processos de encapsulação vêm sendo explorados tradicionalmente na preparação de micro e nanocápsulas contendo os agentes biologicamente ativos como fármacos, alimentos e nutrientes. Dependendo do processo de preparação, as nanoestruturas são classificadas como nanoesferas ou nanocápsulas – enquanto uma nanoestrutura com um fármaco impregnado na sua superfície é chamado de nanoesfera, as partículas contendo a droga no seu interior são chamadas de nanocápsulas (Alonso M J., 2004) e, para aplicações biomédicas, a fase polimérica é biodegradável (De Geest BG., et al., 2009). Durante a última década, vários bio polieletrólitos como polissacarídeos, polipeptídeos ou polinucleotídeos, que são bastante biodegradáveis em meios biológicos, têm sido utilizados para a fabricação dessas cápsulas (Picart C. et al.,2005). Entretanto, após alcançar a região alvo, as estruturas necessitam liberar as fármacos encapsuladas de maneira assistida e/ou controlada. Entre a variedade de processos de liberação de fármacos, aqueles com funcionalidades remotas por um estímulo externo tal como luz (Skirtach, AG.; et al., 2004), ultrassom (Shchukin DG. et al., 2006) e campo magnético (Lu ZH.; et al., 2005) são muito mais interessantes para um controle mais minucioso após administração.

2.1.4 Triptofano

O triptofano, cuja estrutura molecular é apresentatada na figura 3, é um aminoácido essencial, não sintetizado pelo organismo, mas um importante precursor na síntese do neurotransmissor serotonina (Kapczinski et al.; 1998); Estudos recentes mostram que uma combinação entre variáveis genéticas associadas ao L-5 hidroxitriptofano auxiliam uma melhor compreensão sobre a neurobiologia da doença depressão, o que condiciona novos rumos a pesquisa (Neumeister A., 2003).

Uma de suas principais características é que possui uma absorbância na região do visível (Petrovic et al., 2013; Tunna et al., 2013). O quantitativo ingerido na alimentação não consegue permear a membrana hematoencefálica; pois grande

parte é metabolizado e eliminado antes de ser absorvido (Comai et al., 2007), fazendo com que seja um sério candidato envolvido em sistemas de transporte e liberação controlada. Entretanto, um dos fatores principais que nos levaram a essa escolha foi a grande afinidade do triptofano com a quitosana, sua hidrossolubilidade e, de maneira muito importante, sua detectabilidade por uma técnica analítica simples – nesse caso, a espectroscopia de absorção molecular no ultravioleta-visível. É preciso salientar que a concentração do triptofano deveria ser acompanhada, tanto na etapa de incorporação ao nanocompósito, como na fase dos testes de liberação.

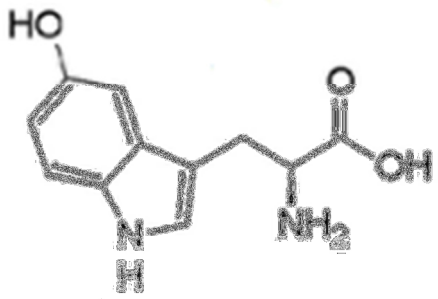

Figura 3. Estrutura química do L-5 hidroxitriptofano
Fonte: Lin Y., Sun X., Yuan Q., Yan Y.; 2014

2. OBJETIVOS

O objetivo geral do trabalho foi o de elaborar nanocompósito magnético dopadas com 5-hidroxitriptofano e testar a habilidade desses nanocompósitos como sistema de liberação controlada do referido princípio ativo em condições diferenciadas de pH.

Os objetivos específicos foram:

1- Propor e otimizar processo para sintetizar, por meio de precipitação em meio homogêneo, nanocompósitos de quitosana com nanopartículas magnéticas de óxido de ferro ;

2- Caracterizar, por meio de diversas técnicas, as propriedades morfológicas, estruturais, químicas e físico-químicas dos nanomateriais sintetizados;

3- Otimizar a adsorção do 5-hidroxitriptofano pelos nanocompósitos sintetizados;

4- Estudar o perfil de liberação do 5-hidroxitriptofano em condições diferenciadas de pH;

CAPÍTULO 2

Artigo Científico

1. APRESENTAÇÃO

O artigo a seguir, intitulado "***One-step synthesis of magnetic chitosan for controlled release of tryptophan***", foi submetido para publicação no *Journal of Magnetism and Magnetic Materials (JMMM),* por ocasião da conferência internacional mais importante da área de carreadores magnéticos, *10th International Conference on the Scientific and Clinical Applications of Magnetic Carriers,* ocorrida em Dresden, na Alemanha, no mês de junho de 2014, onde o referido trabalho foi apresentado. Cabe ressaltar que o periódico JMMM é um dos mais importantes na área de nanomateriais magnéticos aplicados à saúde, tem um fator de impacto igual a 1,83 e é classificado como A2 no QUALIS da Capes, na área interdisciplinar (avaliado em junho de 2014).

O artigo resume os resultados obtidos no trabalho de dissertação de mestrado e mostra a síntese, por meio de precipitação em meio homogêneo, de nanocompósitos de partículas de quitosana de aproximadamente 100 nm, com 25 % em massa de nanopartículas magnéticas de óxido de ferro embutidas (magnetita/maguemita). A eficiência de incorporação de 5-hidroxitriptofano foi de até 80 % em um procedimento simplificado feito em uma única etapa, juntamente com a síntese dos nanomateriais. A caracterização da morfologia, estrutura e superfície foi feita por difração de raios X, microscopia eletrônica de transmissão de alta resolução, espectroscopia de infravermelho, análise termogravimétrica, medidas de magnetização e do potencial zeta. A incorporação e os estudos de liberação do fármaco foram feitos por espectroscopia de absorção no ultravioleta-visível. Estudos da cinética de liberação do 5-hidroxitriptofano em diferentes pHs mostraram que o sistema investigado tem a liberação sensível ao pH do meio e que esse processo de liberação do fármaco é guiado pelo entumescimento e decomposição do polímero.

One-step synthesis of magnetic chitosan for controlled release of tryptophan

Jucély dos Santos Menegucci, Mac-Kedson Medeiros Salviano Santos, Diego Juscelino Santos Dias, Juliano Alexandre Chaker and Marcelo Henrique Sousa*

Universidade de Brasília, Faculdade de Ceilândia, Centro Metropolitano Cj. A Lt. 1, Ceilândia – DF, CEP 72220-900, Brazil

Abstract:

In this work, ~100 nm sized nanoparticles of chitosan embedded with 25 % (w/w) of iron oxide magnetic nanoparticles (magnetite/maghemite) and with a loading efficiency of about 80% for 5-hydroxytryptophan were synthesized, using homogeneous precipitation by urea decomposition, in an efficient one-step procedure. Characterization of morphology, structure and surface were performed by XRD, TEM, FTIR, TGA, magnetization and zeta potential measurements, while drug loading and drug releasing were investigated using UV-vis spectroscopy. Kinetic drug release experiments under different pH conditions revealed a pH-sensitive controlled-release system, ruled by polymer swelling and/or particle dissolution, and that drug release is more efficient in an acidic medium.

Keywords: magnetic nanoparticles, chitosan, nanocomposite, controlled release, tryptophan

1. Introduction

Design and tailoring of controlled release (CR) systems have been extensively studied, in order to enhance drug therapy and increase patient compliance. This has become possible because CR systems can control drug exposure over time, help drugs to pass through physiological barriers, protect drugs from premature elimination, drive drugs to the target site, minimize drug exposure and reduce frequency of administration [1]. For these purposes, various biodegradable polymers have been used in drug delivery research; they can effectively deliver the drug to a target site and thus increase the therapeutic benefit, while minimizing side effects [2]. One of these biopolymers which has attracted attention in the controlled release field is chitosan (CS), a natural polysaccharide that presents low toxicity, improved mucoadhesive features and antimicrobial properties. Moreover, it is low-allergenic and easily removable from the organism. From the chemical point of view, CS presents amine (NH_2) and hydroxyl (OH) groups that are readily available for crosslinking with drugs or biological entities. Despite having these advantages, CS presents physical constraints that limit its adsorption features – weak mechanical properties, low stability in acidic media, low density and high swelling ratios [3] .

Nevertheless, these restrictions can be minimized if the biopolymer is conjugated with another material which brings stimuli-responsive features to the composite. In this context, CS can be combined with magnetic materials which are highly useful in the development of novel stimuli-responsive materials for drug delivery – the presence of magnetic materials gives advantages such as detectability by imaging techniques, controllability by an external magnetic field and thermal heating which has been used to produce tissue ablation or to control drug release [4].

Magnetic nanoparticles (MNPs) are also widely appreciated in biomedical

applications [5] because they present highly effective surface areas, facility to be conjugated with biomolecules and manipulability by an external magnetic field – they also present lower sedimentation rates and improved tissue diffusion. However, due to their chemical nature, MNPs – normally iron oxides – are non-biocompatible and need to be functionalized before biomedical applications. This can be achieved by encapsulating or dispersing them into a biocompatible polymeric matrix [6]. Thus, the combination of MNPs with CS would enhance both materials' characteristics for new applications. In fact, there are several reports of chitosan conjugated with magnetic nanoparticles for different purposes which range from magnetic adsorbents in environmental applications [7] to controlled drug delivery/release [8] and magnetic hyperthermia in the biomedical field [9].

Despite this potentiality, magnetic chitosan as a vehicle for drug release has not been widely explored yet. Moreover, simple and reproducible approaches to fabricate CR systems with magnetic-responsive properties that can provide efficient drug loading, controllable drug release, and imaging capability are highly desirable. To this end, in this work we propose a simple fabrication of a nanocomposite which consists of chitosan structures embedded with magnetic iron oxide nanoparticles as a magnetic-responsive system for the controllable release of drugs. The novelty of this work is that the synthesis route is environmentally friendly and comprises elaboration of the composite and drug loading in only one step. Here, tryptophan (Trp) – which also presents biological importance and pharmaceutical capacities [10] – was chosen for drug loading since it has a great affinity for chitosan; additionally, because it is easily monitored spectrophotometrically, Trp was used as a surrogate small, water-soluble drug.

Thus, using a method of homogeneous precipitation by urea decomposition, efficient one-pot synthesis of a nanocomposite comprising sub-100-nm-sized

nanoparticles of CS embedded with up to about 25 % (w/w) of magnetic nanoparticles and with a loading efficiency of about 80% for 5-hydroxytryptophan could be achieved. Moreover, kinetic drug release experiments under different pH conditions revealed that this is a pH-sensitive controlled-release system and that drug release is more efficient in an acidic medium.

2. Experimental section

All the chemical reagents used in the work were of analytical grade and were used without further purification.

A- Magnetic chitosan (mag@CS)

In a typical procedure, for the synthesis of magnetic chitosan, 1.0 mL of 1 % (w/w) chitosan solution (high purity, Mv 60.000-120.000, from Sigma-Aldrich) – prepared in 1 % (w/w) acetic acid – and 40 mmol of urea were dissolved in 50 mL of water at room temperature. Then, 20 □mol of $FeCl_3 \cdot 6H_2O$ and 10 □mol of $FeCl_2 \cdot 4H_2O$ were mixed uniformly into the solution containing urea and chitosan, in a three-neck flask, and the temperature was brought to 100 ºC under moderate reflux while stirring, for 4 hours. The product was collected and washed several times with water, by magnetic decantation.

B- Tryptophan loading

Two methods were utilized for the incorporation of Trp into magnetic chitosan. In the first approach, 20 mg of lyophilized magnetic chitosan, obtained as described in the section before, was incubated into 50 mL of 5-hydroxitryptophan solution (0.5 mg/mL) for 4 h. In the second method, 25 mg of 5-hydroxitryptophan was mixed with chitosan, urea and iron salts and submitted to a reflux as described in the section before. Solid was separated from supernatant, washed once with water and

lyophilized.

C- Tryptophan release

The release of tryptophan was investigated at constant temperature (25 ºC) using different pH conditions. In a typical procedure, 20 mg of magnetic chitosan loaded with tryptophan was introduced in 5 mL of water. Then, pH of the slurry was adjusted and aliquots of supernatant (magnetically separated) were investigated by UV-vis.

D- Characterization

The size and morphology of the as-prepared materials were examined by high-resolution transmission electron microscopy (HRTEM) using a JEOL 1100 apparatus. X-ray diffraction study was performed on powder samples with a Rigaku – Miniflex 600 diffractometer using radiation of 1.541 Å (40 kV and 30 mA). The room-temperature magnetization curves were obtained using an ADE vibrating sample magnetometer model EV7. Hysteresis loops were performed under applied magnetic fields varying from -18 to 18 kOe at 300 K. A dynamic light scattering analyzer (Malvern Instruments, Zetasizer nano ZS) was used to measure the electrophoretic mobility. FTIR spectra were recorded with crystalline KBr in the range of 3700 - 400 cm^{-1} and resolution of 2 cm^{-1}. Thermogravimetric analyses (TGA) were performed in air flow and with a heating rate of 10 ºC/min up to 600 ºC, in a Shimadzu Thermogravimetric Analyzer model DTG-60. The concentration of loaded tryptophan was measured by determining its concentration in solution, by ultraviolet-visible spectrometry (UV-vis) after and before interaction with magnetic chitosan.

3. Results and Discussion

In the synthesis of magnetic chitosan (mag@CS), as temperature reached about 100 ºC, decomposition of urea takes place and hydroxide concentration increases. In fact, this process generates OH^- homogenously in the solution and, as the urea source is not totally consumed, pH maintains constant at alkaline region [11] as shown in Fig. 1 – the circles represent the pH variation during synthesis. This can be described by reactions (1) and (2).

$$CO(NH_2)_2 + H_2O \longrightarrow CO_2 + 2NH_3 \quad (1)$$

$$NH_3 + H_2O \leftrightarrow NH_4^+ + OH^- \quad (2)$$

After about 30 minutes, a brown gummous colloid started forming and, as time elapsed, this brown precipitate was converted to a black solid. Here, both chitosan and magnetic iron oxide were condensed to form a composite as illustrated in Fig. 1 (the mag@CS structure). Before urea decomposition, the medium was acid and chitosan was solubilized, but precipitated/coacervated when it came in contact with the alkaline solution originated from reactions (1) and (2) [12]. On the other hand, the presence of Fe^{3+} and Fe^{2+} (aqua ions in acid medium) at a molar ratio of 2:1 and the increasing concentration of hydroxide led to the formation of magnetite (Fe_3O_4), according to the chemical reaction $2Fe^{3+} + Fe^{2+} + 8OH^- \longrightarrow Fe_3O_4 \downarrow + 4H_2O$.

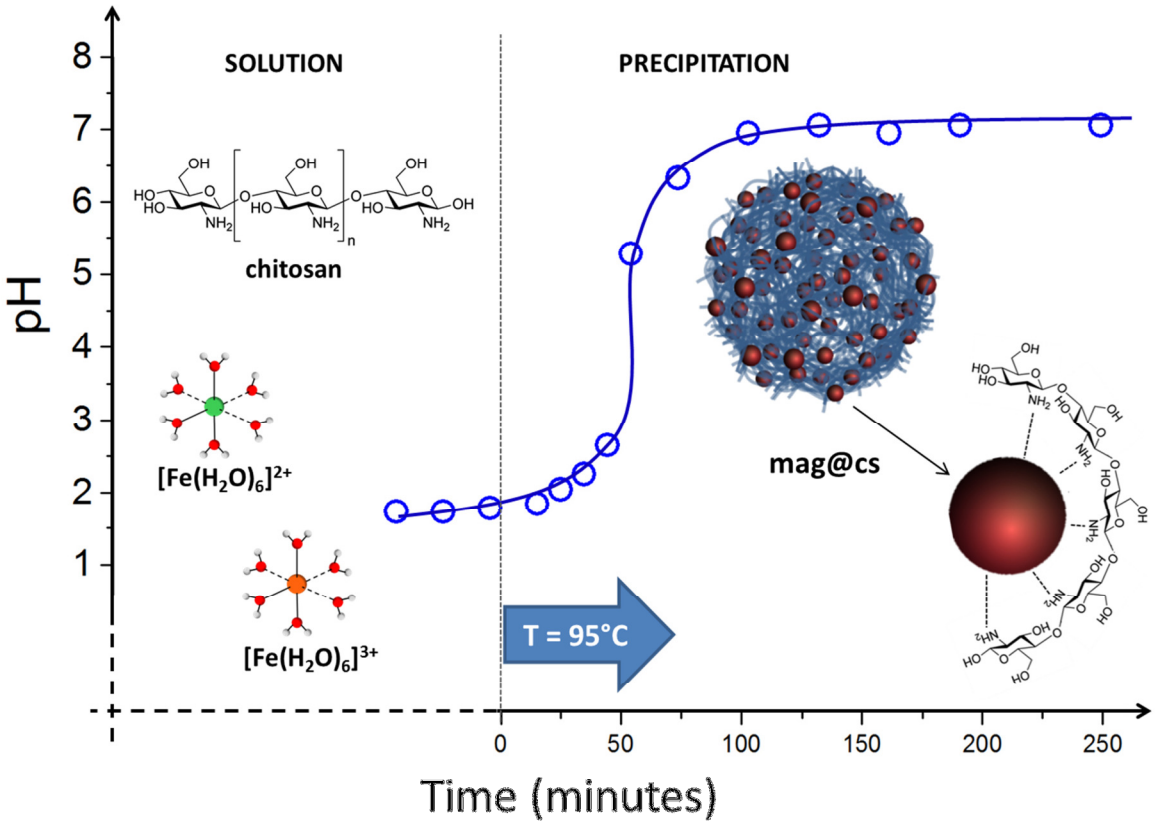

Fig. 1. Schema of synthesis of mag@CS nanocomposites. Circles are the variation of pH as a function of the time of reaction. Before 95 ℃, iron complexes and chitosan coexists in solution. As temperature reaches 95 ℃ and time increases, chitosan polymerizes (blue thread ball) embedded with magnetic iron oxide nanoparticles (red spheres).

XRD pattern of mag@CS sample in Fig. 2 revealed two phases: after indexing the main peaks using Bragg's law and comparing them to the ASTM standards, spinel structure was found, indicating that magnetite and/or maghemite (marked by their indices) should be present in samples synthesized in this work – XRD patterns of magnetite and maghemite are very analogous. When compared with the ASTM lattice parameters for cubic magnetite and maghemite, respectively 0.8396 nm and 0.8347 nm, the intermediary value of lattice parameter determined for our sample (0.836 nm) indicated that magnetite was partially oxidized to maghemite (γ-Fe_2O_3). This can be explained by the fact that preparations were carried out in air, an

oxidizing environment, so that magnetite was partially converted to maghemite [13]. The other phase identified from XRD pattern on Fig. 2 was the chitosan. In fact, the broad peak at 2□ ~ 20º is typical of polymerized chitosan [14].

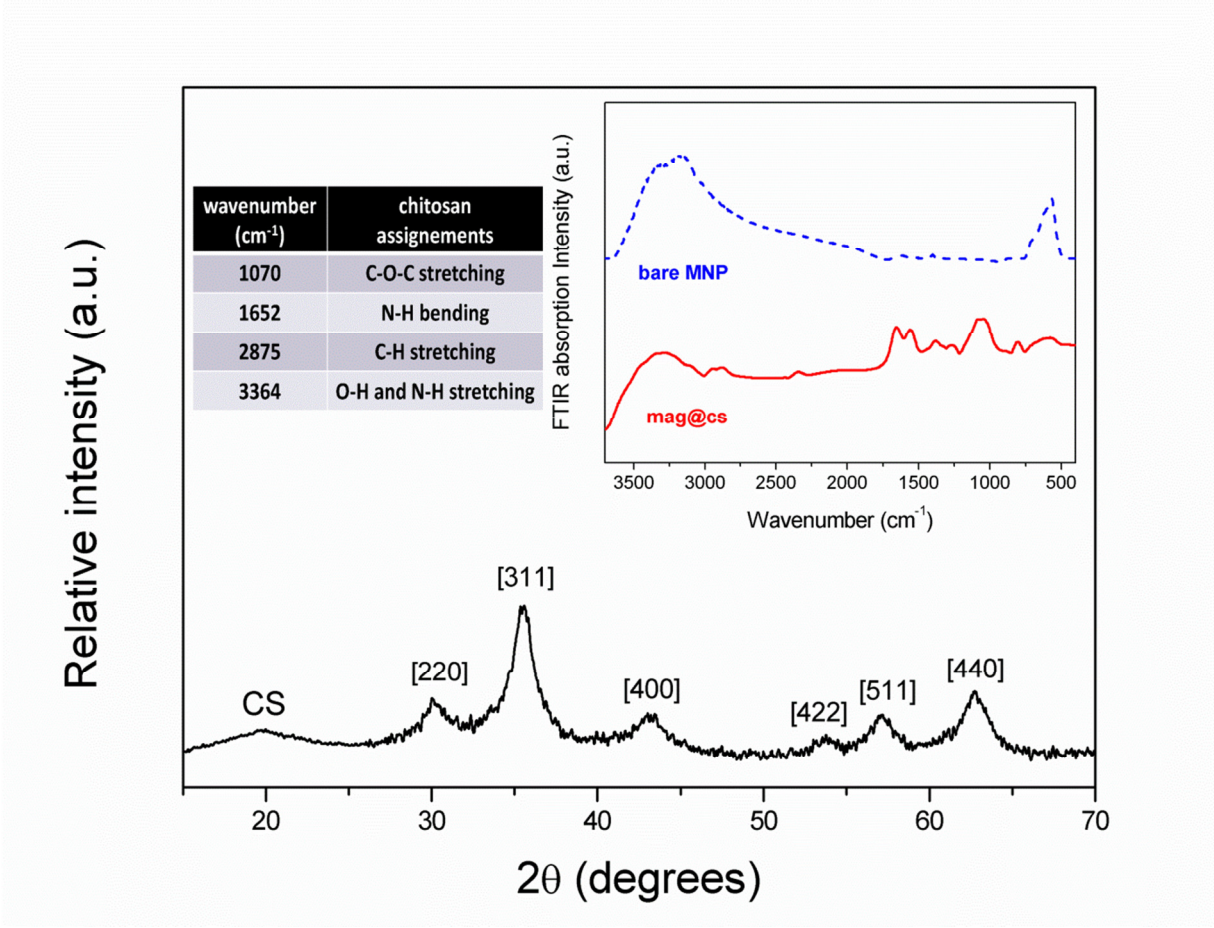

Fig. 2. X-ray diffraction pattern of mag@CS composite. Main diffraction peaks of the iron oxide (magnetite and/or maghemite) are identified by their indexes and reflection of chitosan is identified by CS. At the top right corner, the FTIR spectra of bare magnetic nanoparticles (dashed blue) and mag@CS sample (red). Inset table lists the main FTIR transitions for pure chitosan.

In spite of XRD identifying both the polymeric and inorganic magnetic phases, this technique is not able to prove that they are interacting to form a composite. FTIR was therefore utilized to study the synthesized materials. The insets of Fig. 2 shows the FTIR spectra corresponding to the mag@CS composite and to the bare magnetic nanoparticles – the polymer was eliminated after washing the composite with acetic

acid and water – and a table with the main infrared transitions observed in the FTIR spectra of pure chitosan. The IR bands around 580 cm^{-1}, attributed to ferrite Fe-O absorptions, as well as the absorption at 3345 cm^{-1}, which is related to OH streching from oxide surface, are present in both samples [15]. Moreover, since most of the vibrational modes that correspond to pure chitosan – the C-O-C stretching vibrations at 1070 cm^{-1}; N-H bending at 1652 cm^{-1}; C-H stretching at 2875 cm^{-1} and O-H and N-H stretching at 3364 cm^{-1} – are shifted to lower wavenumbers and as composites were exhaustively washed after synthesis, FTIR results strongly indicate that chitosan is coordinated to the iron ions on the magnetic nanoparticles via nitrogen groups [16] as illustrated at the bottom right corner of Fig. 1.

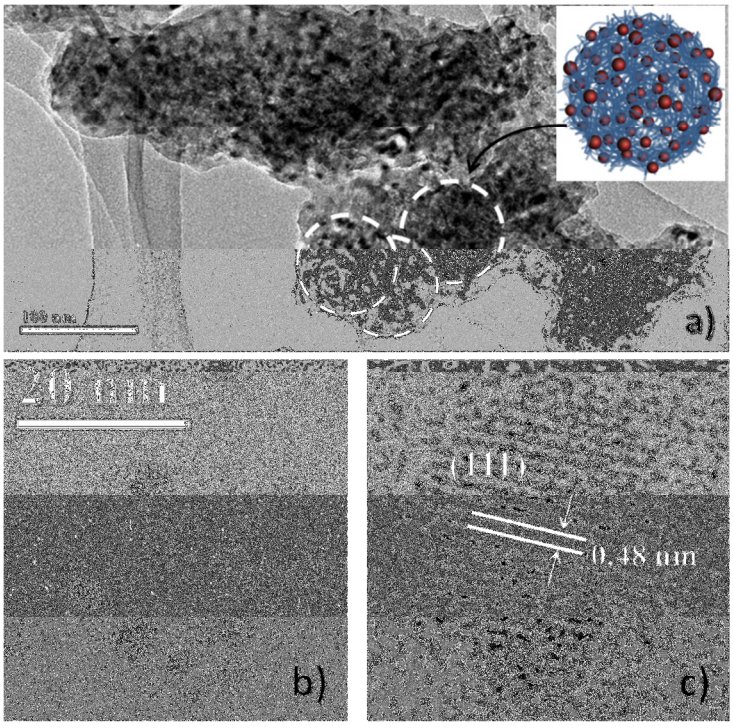

Fig. 3. HRTEM images of mag@CS composite. In (a) white dashed circles delimit some nanostructures in the agglomerate. Magnification showing magnetic nanoparticles embedded in the chitosan polymer (b) and lattice fringes of iron oxide (c).

Despite being highly aggregated on sample-holder grids, from HRTEM analysis it was possible to identify sub-100-nm nearly spherical polymeric structures of chitosan with inlaid magnetic iron oxide (magnetite/maghemite) nanoparticles in our samples (see Fig. 3). The higher magnification of the sample (insets (b) and (c)) revealed that magnetic structures were sub-10-nm sized and that the lattice fringes (~0.48 nm) observed agree well with the distance between the (111) lattice planes, common to both iron oxides.

Dynamic light scattering measurements were employed to study the interface of nanocomposites with solution. In this way, samples were dispersed at different pH and the zeta potential was measured. Dependence of zeta potential on the pH, for sample mag@CS, is shown in Fig. 4 (hexagon dots). In acidic medium, nanocomposites are positively charged and, as pH increases, this charge decreases and becomes negative, after passing through zero, at pH ~ 8. This can be understood by taking into account the pH surface dependence characteristics of the chitosan polymer and those of magnetic nanoparticles. For bare MNPs, the dependence of surface charge on the pH is already well known and shows that for extreme pH values, surface charge reaches the maximum, while when close to neutral pH the surface charge is very small. As schematized in Fig. 4, the MNP surface (MNP◗) behaves as a diprotic acid, leading to three kinds of surface sites where most of them are MNP◗–OH_2^+ in strong acidic medium, MNP◗–O^- in strong basic medium and MNP◗–OH, the intermediate amphoteric sites, in the neutral region [17]. On the other hand, chitosan is a polysaccharide that presents a low electrical charge in neutral and basic pH conditions, but it is positively charged in more acidic medium [18]. This is due to the fact that free amine groups on the chitosan surface (CS◗) follow the chemical equilibrium CS◗–NH_3^+ + H_2O ⇆ CS◗–NH_2 + H_3O^+. Thus, considering that the chitosan particle surface behaves like a

monoprotic acid, the molar fraction of CS◗–NH_3^+ will be equal $\left[H_3O^+\right]/\left(\left[H_3O^+\right]+K_a^{CS}\right)$ and the fraction of CS◗–NH_2 will be $K_a^{CS}/\left(\left[H_3O^+\right]+K_a^{CS}\right)$, where K_a^{CS} is the acid dissociation constant of chitosan (~ 5 × 10^{-7} [19]). Using this mean value of K_a^{CS}, both molar fractions were also plotted on the graph of Fig. 4 and are shown by red curves. The speciation diagrams for MNPs – i.e. the molar fractions of MNP◗–OH_2^+, MNP◗–OH and MNP◗–O^- – are also represented by the blue curves in the graph.

Thus, it seems that surface features of nanocomposite mag@CS are ruled mainly by the amino-groups of chitosan but are also (less) governed by the surface of iron oxide nanoparticles exposed to the solution. In summary, the positive saturation of charge at lower pH is due to both polymer and MNP protonation. As neutrality is achieved, inorganic and organic phases tend to be discharged. In particular, the low negative charge observed in alkaline medium could be attributed to the MNP◗–O^- species, since chitosan presents no charges (CS◗NH_2) at these pHs, or could be due to the formation of the negatively charged species (CS◗NH_2OH^-).

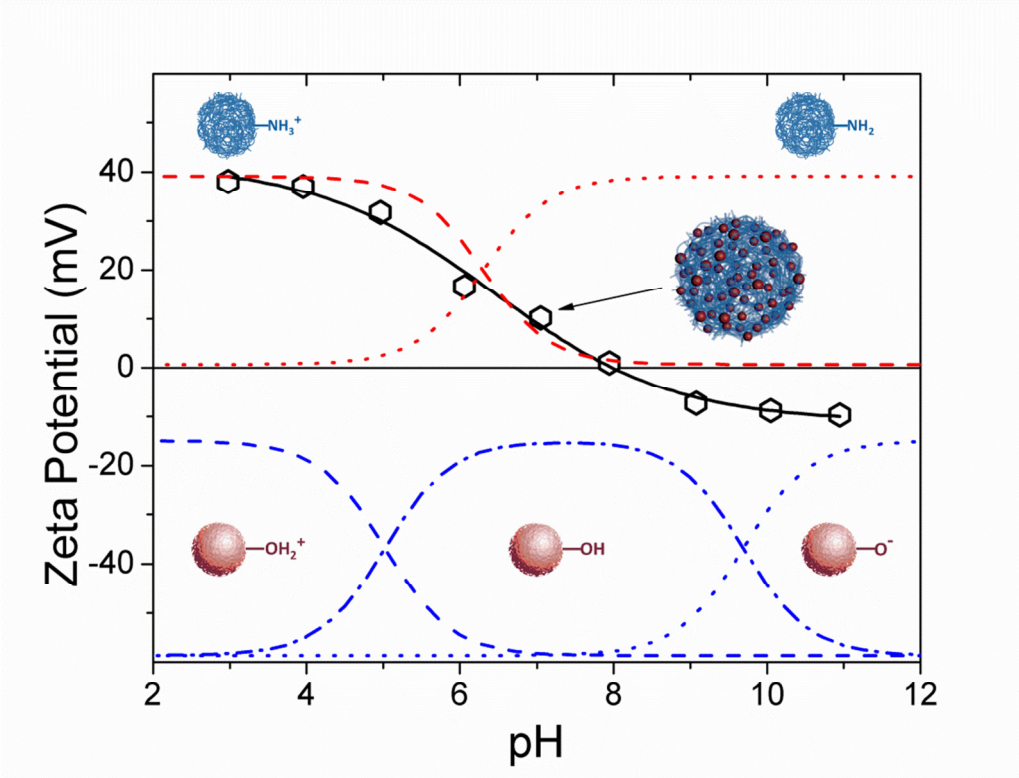

Fig. 4. Zeta potential variation as a function of the pH solution (hexagons) for mag@CS – the black full line is a guide to the eyes. The variation of the molar fraction, as a function of pH, of CS◗–NH_2 and CS◗–NH_3^+ species for pure chitosan is represented by the red dashed and dotted lines, respectively. For magnetic nanoparticles, molar fractions of species MNP◗–OH_2^+, MNP◗–OH and MNP◗–O^- are represented, respectively, by the blue dashed, dot-dashed and dotted lines.

Moreover, taking into account the speciation diagrams shown in Fig. 4, and since synthesis occurs in weak alkaline medium, one infers that interaction of chitosan with MNP is mainly done by the species CS◗NH_2 and MNP◗–OH, through complexation of iron ions on the MNP surface by amino-groups on chitosan, corroborating FTIR observations and, as expected, reflecting the high stability of the iron-amine complexes [20].

For estimation of the mass percentage of MNPs on the nanocomposite, thermogravimetric analysis was used. Thus, most of the loss of mass presented by the mag@CS sample in Fig. 5 is attributed to the thermal decomposition of chitosan, with a first region of loss of mass that occurs at lower temperatures, due to the release of water. For pure chitosan, the maximum weight loss was about 87.5%. The MNPs also presented a loss of mass which mostly originated from free and chemically bonded water. Here, this loss was evaluated at about 4.6 % and its TGA curve is presented in the inset of Fig. 5. Bare MNP were obtained after washing the mag@CS sample with acetic acid solution several times, by magnetic decantation. Thus, for estimating the mass percentage of magnetic material on the composite, the losses of mass from pure chitosan and from bare MNPs were subtracted from the loss of mass of mag@CS (41.7%), yielding a magnetic content of 24.6%.

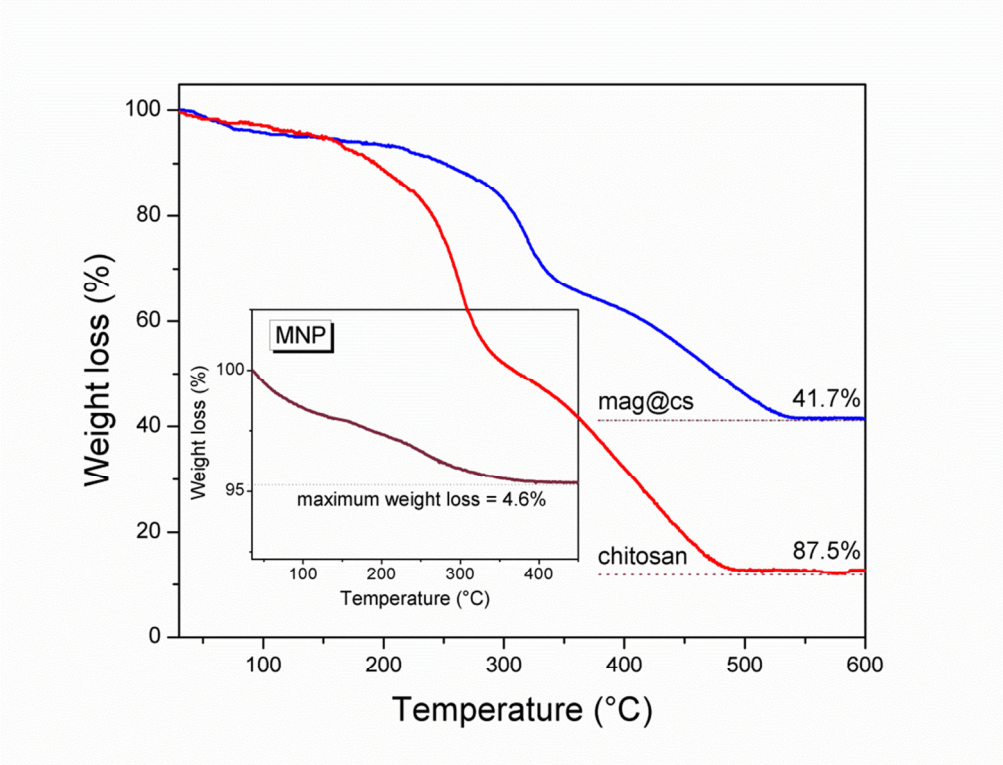

Fig. 5. Thermograms of mag@CS (blue) and pure chitosan (red) samples. The inset shows the weight loss observed in pure iron oxide nanoparticles.

Magnetization measurements were performed for evaluating the counterparts of polymeric coating and magnetic iron oxide nanoparticles on the magnetic properties of the synthesized nanocomposite, which presents macroscopic features of magnetism as shown in inset (a) of Fig. 6. The room temperature magnetization curve for the mag@CS sample shown in this figure reveals that the synthesized composite presents a saturation magnetization of about 11.5 emu/g and that the magnetic properties of the composite originated mainly from MNPs, since chitosan is a diamagnetic material, as presented in the magnetization curve of pure chitosan in inset (b). Moreover, MNPs displayed features of superparamagnetism such as negligible remanence and coercivity, observed in hysteresis loops – see inset (c), which shows the magnetization data at low field range.

Furthermore, if one normalizes magnetization only by the mass of the

magnetic part, estimated from TGA analysis, saturation magnetization of the mag@CS sample is about 48 emu/g, typical of sub-10-nm sized magnetite/maghemite nanoparticles, as found by HRTEM measurements, with little difference from the bulk values – probably due to cationic redistribution [21] and surface and size-finite effects that affect the magnetization characteristics of nanosized grains [22,23].

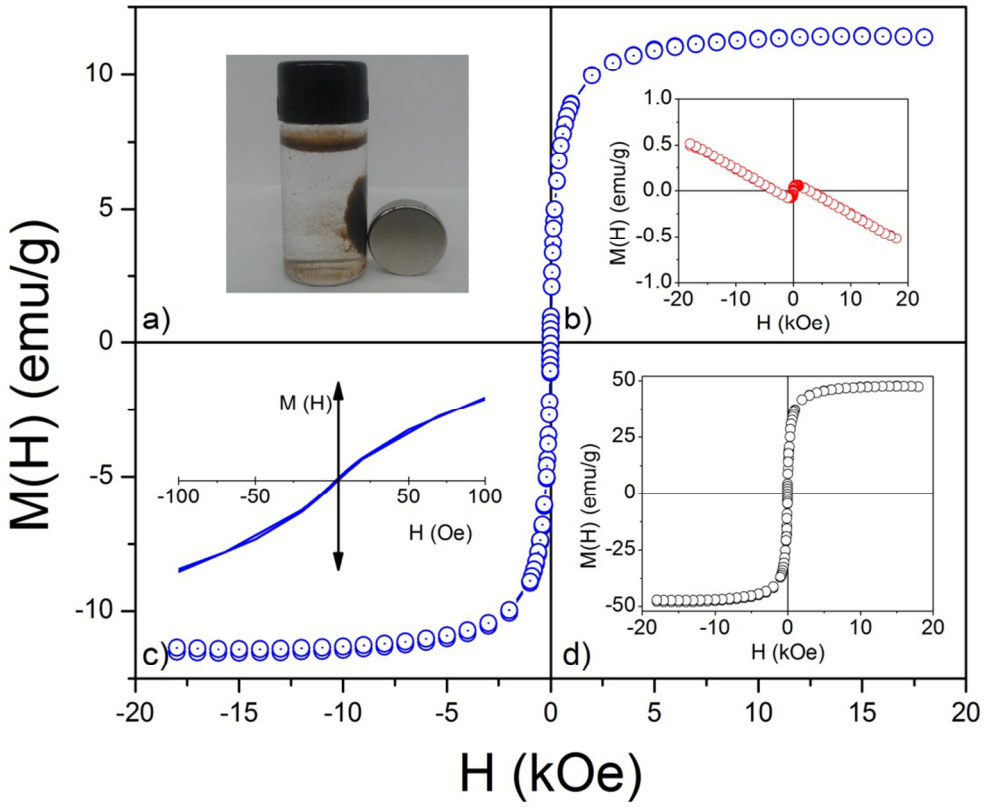

Fig. 6. Magnetization hysteresis loop at room temperature for sample mag@CS (blue circles). Picture of magnetic chitosan under action of a permanent magnet (a). Magnetization curve at room temperature of pure chitosan (b). Magnetization data of mag@CS at low field range (c) and normalized only by the iron oxide mass (d).

For samples loaded with tryptophan, the quantity of amino acid incorporated in

the composite structure was estimated by UV-vis analysis, comparing the spectra of supernatant with a calibration curve, after (dashed lines) and before (full lines) loading, as shown in Fig. 07. From this analysis, the mass percentage of Trp incorporated on the composite when Trp was added during synthesis (81.5 %, w/w) was higher than Trp loaded after magnetic composite synthesis (18.5 %, w/w). This can be explained by the fact that, if it is added during synthesis, Trp is embedded into the matrix by crosslinking within the polymeric structure or adsorbed onto the surface by chemical/physical interactions. In the case of Trp incorporated after synthesis of mag@CS, surface adsorption is preponderant over embedding.

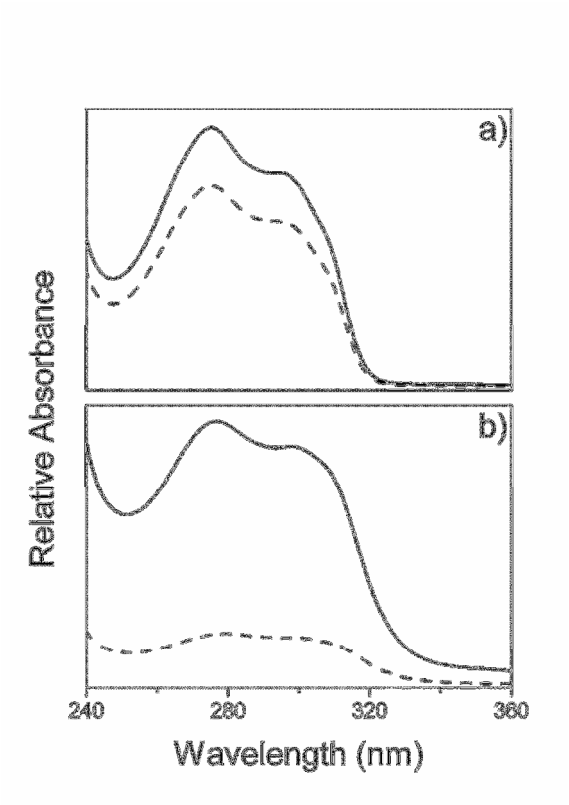

Fig. 7. UV-vis spectra of supernatant before (full lines) and after (dashed lines) interaction of mag@CS with tryptophan during drug loading process. In (a) Trp was loaded after magnetic composite synthesis and in (b) Trp was added during synthesis.

In order to investigate the effect of pH on the kinetics of drug release, the sample with Trp incorporated during synthesis (i.e. with higher loading efficiency) was incubated in aqueous buffers at pH 3.5 and pH 8.5 at 25 ºC. The curves of cumulative release as a function of time (Fig. 8) show that less than 7 % and almost 90 % of Trp was released after 4 h of incubation, respectively, at pH 8.5 and pH 3.5. In both cases, the release rate is more important during the initial minutes and tends to stabilize as time advances. Here, drug release is higher in acidic media since solubility of CS increases as pH decreases, improving the diffusion of Trp by erosion of polymer. At pH 8.5, chitosan is practically insoluble, so swelling seems to be the main mechanism of drug release.

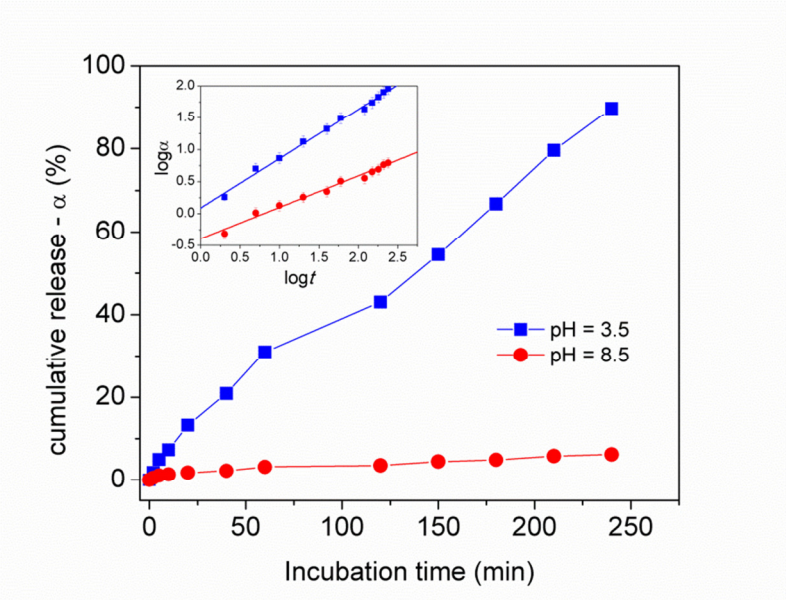

Fig. 8. Cumulative release of Trp as a function of time for mag@CS samples at different pHs. The inset is a log-log plot and full lines are the linear fit of data.

Moreover, the Ritger and Peppas model [24] was applied to investigate the characteristics of drug release and confirms the previous qualitative observations. In this empirical model, the fraction of drug released (□) at a time *t* is proportional to kt^n, where *k* is the release rate constant and *n* is the release exponent. The linear form of this equation (see the inset of Fig. 8) allowed, through its intercept and slope, the *k*

and *n* parameters that are listed in Table 1 to be determined for the different experimental conditions. On the one hand, the difference in release rate constants as a function of incubation condition indicates that our nanocomposite is a pH-sensitive release system, and this rate is higher in an acidic medium.

Table 1. Drug release kinetic data obtained from fitting experimental data to Ritger-Peppas equation

pH	maximal release (%)	release rate constant (*k*)	release exponent (*n*)	R^2
3.5	89.0	1.2	0.77	0.991
8.5	6.3	0.4	0.45	0.993

On the other hand, according to the release exponents, at pH = 8.5 drug transport slightly deviate from the Fickian model (*n* = 0.5) of swelling-controlled release. At pH = 3.5, the medium surrounding the nanocomposite may dissolve the polymer such as the rate that controls the drug release can be increased (i.e. dissolution competes with swelling) and anomalous drug transport is observed. Indeed, different *n* values and deviation from Fickian diffusion model, that compare our results, were already observed for drug loaded chitosan and were related to the cross-linking degree [25] and drug loading concentration [26]. Moreover, the irregular shape and high polydispersity of samples can contribute to the variation of release characteristics [24].

4. Conclusions

Using homogeneous precipitation with urea, nanoparticles of chitosan of about 100 nm, embedded with magnetic nanoparticles of magnetite/maghemite of ~5 nm could be synthesized. One of the advantages of this procedure was that a selected drug (tryptophan) could be efficiently incorporated during the synthesis of the nanomaterial in a simple and one-step procedure. The release of tryptophan has been shown time and pH-dependent and seems to be modulated by diffusion arising from swelling and/or dissolution of polymer. Due to the chemical nature of the components of composite (chitosan and iron oxides) drug loading could be extended to a series of drugs different of tryptophan and, owing to its magnetization features, composite could be easily manipulated by an external magnetic field to be delivered and/or concentrated in a determined region, improving the efficiency of the release purposes. Moreover, decomposition/swelling of chitosan is temperature dependent so that thermal heating (magneto hyperthermia) could be utilized to better control drug release. In this way, the synthesis route presented here has great potential as high efficiency, cost effective and environment-friendly materials for the elaboration of stimuli-responsive materials for applications in the field of controlled drug-release systems.

Acknowledgement

The authors gratefully acknowledge financial support from the Conselho Nacional de Desenvolvimento Científico e Tecnológico (CNPq) and the Fundação de Apoio à Pesquisa do Distrito Federal (FAPDF)

References

[1] P.H.L. Tran, T.T.D. Tran, J.B. Park, B.J. Lee, Controlled Release Systems Containing Solid Dispersions: Strategies and Mechanisms, Pharm Res-Dordr, 28 (2011) 2353-2378.

[2] K.S. Soppimath, T.M. Aminabhavi, A.R. Kulkarni, W.E. Rudzinski, Biodegradable polymeric nanoparticles as drug delivery devices, J Control Release, 70 (2001) 1-20.

[3] S.A. Agnihotri, N.N. Mallikarjuna, T.M. Aminabhavi, Recent advances on chitosan-based micro- and nanoparticles in drug delivery, J Control Release, 100 (2004) 5-28.

[4] J.O. You, D. Almeda, G.JC. Ye, D. T. Auguste, Bioresponsive matrices in drug delivery, J Biomed Eng, 4 (2010) 15. (doi:10.1186/1754-1611-4-15).

[5] Q.A. Pankhurst, N.T.K. Thanh, S.K. Jones, J. Dobson, Progress in applications of magnetic nanoparticles in biomedicine, J Phys D Appl Phys, 42 (2009).

[6] L.H. Reddy, J.L. Arias, J. Nicolas, P. Couvreur, Magnetic Nanoparticles: Design and Characterization, Toxicity and Biocompatibility, Pharmaceutical and Biomedical Applications, Chem Rev, 112 (2012) 5818-5878.

[7] D.H.K. Reddy, S.M. Lee, Application of magnetic chitosan composites for the removal of toxic metal and dyes from aqueous solutions, Adv Colloid Interfac, 201 (2013) 68-93.

[8] T.S. Anirudhan, S.S. Gopal, S. Sandeep, Synthesis and characterization of montmorillonite/N-(carboxyacyl) chitosan coated magnetic particle nanocomposites for controlled delivery of paracetamol, Appl Clay Sci, 88-89 (2014) 151-158.

[9] K.H. Bae, M. Park, M.J. Do, N. Lee, J.H. Ryu, G.W. Kim, C. Kim, T.G. Park, T. Hyeon, Chitosan Oligosaccharide-Stabilized Ferrimagnetic Iron Oxide Nanocubes for Magnetically Modulated Cancer Hyperthermia, Acs Nano, 6 (2012) 5266-5273.

[10] A.P.N. Majumdar, Tryptophan Requirement for Protein-Synthesis - a Review, Nutr Rep Int, 26 (1982) 509-522.

[11] L. Gordon, M. L. Salutsky and H. H. Willard, Precipitation from Homogeneous Solution, Wiley, New York, 1959.

[12] K. Kaibara, T. Okazaki, H.B. Bohidar, P.L. Dubin, pH-induced coacervation in complexes of bovine serum albumin and cationic polyelectrolytes, Biomacromolecules, 1 (2000) 100-107.

[13] A.L. Drummond, N.C. Feitoza, G.C. Duarte, M.J.A. Sales, L.P. Silva, J.A. Chaker, A.F. Bakuzis, M.H. Sousa, Reducing Size-Dispersion in One-Pot Aqueous Synthesis of Maghemite Nanoparticles, J Nanosci Nanotechno, 12 (2012) 8061-8066.

[14] M.A. Morales, E.C.D. Rodrigues, A.S.C.M. de Amorim, J.M. Soares, F. Galembeck, Size selected synthesis of magnetite nanoparticles in chitosan matrix, Appl Surf Sci, 275 (2013) 71-74.

[15] J.C. Rubim, M.H. Sousa, J.C.O. Silva, F.A. Tourinho, Raman spectroscopy as a powerful technique in the characterization of ferrofluids, Braz J Phys, 31 (2001) 402-408.

[16] H.Y. Huang, Y.T. Shieh, C.M. Shih, Y.K. Twu, Magnetic chitosan/iron (II, III) oxide nanoparticles prepared by spray-drying, Carbohyd Polym, 81 (2010) 906-910.

[17] N.C. Feitoza, T.D. Goncalves, J.J. Mesquita, J.S. Menegucci, M.K.M.S. Santos, J.A. Chaker, R.B. Cunha, A.M.M. Medeiros, J.C. Rubim, M.H. Sousa, Fabrication of glycine-functionalized maghemite nanoparticles for magnetic removal of copper from wastewater, J Hazard Mater, 264 (2014) 153-160.

[18] T. Sannan, K. Kurita, Y. Iwakura, Studies on Chitin .2. Effect of Deacetylation on Solubility, Makromol Chem, 177 (1976) 3589-3600.

[19] G.A.F. Roberts, Chitin Chemistry, MacMillan, London, 1992.

[20] Y.L. Wang, B.Q. Li, Y. Zhou, D.C. Jia, In Situ Mineralization of Magnetite Nanoparticles in Chitosan Hydrogel, Nanoscale Res Lett, 4 (2009) 1041-1046.

[21] J.A. Gomes, M.H. Sousa, F.A. Tourinho, J. Mestnik, R. Itri, J. Depeyrot, Rietveld structure refinement of the cation distribution in ferrite fine particles studied by X-ray powder diffraction, J Magn Magn Mater, 289 (2005) 184-187.

[22] C.R. Alves, R. Aquino, M.H. Sousa, H.R. Rechenberg, G.F. Goya, F.A. Tourinho, J. Depeyrot, Low temperature experimental investigation of finite-size and surface effects in CuFe(2)O(4) nanoparticles of ferrofluids, J Metastab Nanocryst, 20-21 (2004) 694-699.

[23] J.F. Saenger, K.S. Neto, P.C. Morais, M.H. Sousa, F.A. Tourinho, Investigation of the anisotropy in frozen nickel ferrite ionic magnetic fluid using magnetic resonance, J Magn Reson, 134 (1998) 180-183.

[24] N.A. Peppas, J.J. Sahlin, A Simple Equation for the Description of Solute Release .3. Coupling of Diffusion and Relaxation, Int J Pharm, 57 (1989) 169-172.

[25] S.A. Agnihotri, T.M. Aminabhavi, Controlled release of clozapine through chitosan microparticles prepared by a novel method, J. Control. Release 96 (2004) 245– 259.

[26] S.G. Kumbar, A.R. Kulkarni, T.M. Aminabhavi, Crosslinked chitosan microspheres for encapsulation of diclofenac sodium: effect of cross-linking agent, J. Microencapsulation 19 (2002) 173– 180.

CAPÍTULO 3

Discussão geral e Conclusões

1. Discussão Geral

A proposta inicial do trabalho de mestrado era a de preparar um sistema de liberação controlada que envolvesse a quitosana, já conhecidamente eficiente nessa área de transporte de fármacos e nanomateriais magnéticos, também amplamente utilizados na veiculação de princípios ativos e com suas características de manipulabilidade por um campo magnético externo. Dentre todos os distintivos que um compósito desse tipo poderia oferecer, conforme já discutido nas outras sessões, o principal objetivo desse trabalho era o de se obter um nanomaterial cujas propriedades de liberação de fármacos pudessem ser moduladas por estímulos externos. Dessa maneira, a solubilidade e o potencial de entumescimento da quitosana poderiam responder prontamente às variações de pH do meio e, como parâmetro que induziria maior tecnologia ao compósito, a degradabilidade térmica da quitosana, associada ao fato de que as nanopartículas poderiam ser aquecidas remotamente pela aplicação de um campo magnético alternado externo, permitiriam um controle mais refinado dessa liberação. Além disso, as inegáveis contribuições da manipulabilidade e detectabilidade das nanopartículas magnéticas e da biocompatibilidade da quitosana, certamente, nos trariam um material de tecnologia de ponta.

Na verdade, essa ideia da quitosana magnética já existia e suas aplicações iam desde seu uso para remoção magnética de contaminantes – a quitosana é um ótimo suporte adsorvente e as nanopartículas magnéticas ali inseridas permitem uma "filtração" magnética – e até na área médica. Entretanto, o papel da quitosana era, principalmente, o de funcionalizar as nanopartículas magnéticas, como um polímero biocompatível. A literatura sobre o uso de nanocompósito magnético em magneto-hipertermia e carreamento de fármacos é, portanto, bastante escasso e necessita ainda ser explorado. Dessa maneira, tendo em vista a relevância do tema e as expertises e a estrutura laboratorial do Grupo de Pesquisa em Materiais e Nanobiotecnologia (GPMNb), resolvemos explorar uma das vertentes dessa área.

Foi verificado na literatura que existiam diversas maneiras de preparar essas nanocompósito magnético. Na maioria dos casos, nanopartículas magnéticas eram sintetizadas e, em um procedimento posterior, dispersas de maneira individual ou múltipla no polímero. Poucos trabalhos mostravam a síntese conjunta das duas fases e, nas escassas referências em que fármacos eram incorporados às

nanocompósito magnético, isso era feito em uma terceira etapa e com baixo rendimento.

Foi nessa direção que buscamos uma nova metodologia mais simples, eficiente, e que pudesse ser feita em uma única etapa, por uma via mais econômica e menos agressiva ao meio ambiente. Além disso, buscamos um fármaco que pudesse servir de modelo para esse sistema de liberação. Nesse caso, o triptofano foi escolhido. Cabe ressaltar que o triptofano é um aminoácido essencial ao organismo e apresenta atividade farmacológica importante. Além disso, apresenta certas dificuldades para transpor algumas barreiras fisiológicas, fazendo com que seja um sério candidato envolvido em sistemas de transporte e liberação controlada. Entretanto, um dos fatores principais que nos levaram a essa escolha foi a grande afinidade do triptofano com a quitosana, sua hidrossolubilidade e, de maneira muito importante, sua detectabilidade por uma técnica analítica simples – nesse caso, a espectroscopia de absorção molecular no ultravioleta-visível. É preciso salientar que a concentração do triptofano deveria ser acompanhada, tanto na etapa de incorporação ao nanocompósito, como na fase dos testes de liberação.

Assim, o artigo do capítulo anterior mostra os principais resultados obtidos nesse mestrado e passíveis de publicação. Entretanto, é preciso lembrar que para cada etapa desse trabalho uma investigação exaustiva foi feita e, para otimização das sínteses e caracterizações, várias repetições de testes e experimentos foram feitas. A seguir, é feita uma análise qualitativa, cronologicamente contextualizada, dos principais resultados encontrados. O artigo, entretanto, traz subsídios quantitativos e bibliográficos para esses resultados.

Cronologicamente, começamos com a síntese dos nanocompósitos. Nesse sentido, os primeiros experimentos foram feitos com base nas propriedades de condensação, tanto das nanopartículas magnéticas quanto da quitosana, em se condensarem em meios alcalinos. De maneira simples, soluções de quitosana e de Fe^{2+} e Fe^{3+} foram misturadas em meio ácido e, em seguida, o pH foi elevado. Como previsto, formou-se um precipitado contendo quitosana e óxido de ferro (magnetita). Porém, análises microscópicas mostraram que as partículas do compósito formado eram micrométricas e que a dispersão em tamanho era muito alta. Além disso, esse método já tinha sido reportado em literatura e rendia resultados similares. A maior inovação desse trabalho está no método de síntese inédito para quitosana

magnética: foi utilizada a técnica de precipitação em meio homogêneo para obtenção dos nanocompósitos. Nesse caso, o agente precipitante (OH^-) é gerado de maneira homogênea e controlada, por um fator externo (temperatura), a partir de uma fonte de matéria prima (ureia). Após estudo do comportamento do pH em função da temperatura e tempo, foram estabelecidas condições ótimas da relação da concentração de ureia e de quitosana/metais. Esse tipo de síntese permite comandar a supersaturação relativa do meio e, assim, maior controle das etapas de formação de um precipitado, que são nucleação e crescimento cristalino. Como resultado, nanopartículas de quitosana de aproximadamente 100 nm foram obtidas. Na razão de reagentes utilizada, incrustradas no polímero, de maneira homogênea, nanopartículas magnéticas de óxido de ferro (de cerca de 5 nm) foram formadas, em uma concentração de aproximadamente 25 % em massa. Essa composição era facilmente separada da solução com ajuda de um ímã e, visivelmente, se podia notar a fase volumosa da quitosana no compósito.

Com o sucesso da síntese, o material foi então caracterizado por diversas técnicas. A difração de raios X mostrou a coexistência das duas fases, quitosana e óxido de ferro. A espectroscopia de absorção molecular no infravermelho provou a interação entre a fase polimérica e a inorgânica, principalmente via complexação dos grupos amina da quitosana aos íons metálicos da superfície das nanopartículas magnéticas. A microscopia eletrônica de transmissão elucidou a morfologia (aproximadamente esférica) das nanopartículas do compósito, assim como sua dimensão (~100 nm) e provou o modelo de nanopartículas magnéticas distribuídas homeogeneamente no interior da fase polimérica. Também comprovou a estrutura cristalina, morfologia e dimensão das mesmas.

A análise de espalhamento de luz e potencial zeta permitiram caracterizar o comportamento da superfície do compósito em solução. Foi possível concluir que as cargas e o comportamento coloidal do material sintetizado eram regidos não só pelas propriedades de superfície das nanopartículas magnéticas, mas, principalmente, pelas da quitosana. Em meio neutro e levemente ácido, a protonação de ambas as fases faz com que as nanopartículas sejam positivamente carregadas, ao passo que, em meios levemente alcalinos, a carga de superfície é originada dos grupamentos ($-NH_3^+$) da quitosana. Em meios mais básicos as espécies desprotonadas são majoritárias e a estabilidade coloidal diminui.

Por análise termogravimétrica, pôde-se estimar a razão entre a massa de óxido magnético e nanocompósito, de cerca de 25 % em massa e, de acordo com as medidas de magnetização, um comportamento superparamagnético foi observado para o nanocompósito. Ao se descontar a massa da quitosana, diamagnética, a magnetização das nanopartículas foram similares a de materiais de mesma dimensão e composição, em que efeitos de tamanho e superfície governam as características magnéticas. Como análise prática, foi observado a rápida resposta do compósito frente a um magneto, o que propiciou sua manipulação externa com ajuda de um ímã. Essas características também evidenciam a factibilidade do seu uso em magneto-hipertermia.

Para análise da eficiência de incorporação do triptofano ao nanocompósito, duas metodologias foram testadas: uma convencional, onde a quitosana magnéticas era mergulhada em uma solução contendo o aminoácido e outra, em que o triptofano era adicionado juntamente com os metais e quitosana, na síntese do nanocompósito. As concentrações do triptofano foram medidas por espectroscopia de absorção molecular no ultravioleta-visível antes e depois da interação do mesmo com o sólido. Os resultados mostraram que quando o triptofano era incorporado durante a síntese dos nanomateriais, sua incorporação era quase cinco vezes maior que quando era adsorvido ao nanocompósito já sintetizado. Isso nos levou a utilizar o segundo procedimento proposto, de maior rendimento, para estudos da liberação controlada do triptofano.

Como não haveria tempo hábil para estudar a liberação do fármaco utilizando a magneto-hipertermia como parâmetro de estimulação externa, experimentos do perfil de liberação foram feitos em função do pH do meio. Nesse caso, quantidades conhecidas de nanocomósito com o aminoácido incorporado foram incubadas a temperatura constante (25 ºC) em dois diferentes pHs, 3,5 e 8,5. A concentração cumulativa de triptofano, medida durante o tempo, mostrou que há uma rápida liberação do mesmo nos minutos iniciais e que tende a estabilizar em algumas horas. Isso é mais notório em pH básico, mas mais proeminente em pH ácido. Para compreensão da cinética de liberação, um modelo matemático comumente empregado para essas situações foi empregado. Nesse modelo, a fração de fármaco liberado é proporcional a kt^n, em que k é a taxa de liberação e n e um fator empírico, expoente do tempo t. O ajuste das curvas para os diferentes pHs

mostraram que a taxa de liberação é maior em meio ácido e que, de acordo com os valores de *n*, a liberação do triptofano não deve ser controlada unicamente pelo entumescimento da quitosana, mas pela adsorção/dessorção de superfície e, em meio ácido, principalmente pela dissolução da estrutura do compósito. De toda forma, foi comprovado que o sistema elaborado é pH-sensível e, com um ajuste mais refinado de pH seria possível controlar melhor a taxa de liberação do triptofano em função do tempo.

Mesmo que não tenha feito parte do foco principal, um trabalho secundário foi desenvolvido nessa etapa de mestrado. Dessa maneira, pôde-se participar da equipe que desenvolveu nanomaterial para remoção magnética de contaminantes em amostras de água contaminada. Essa oportunidade foi muito importante, uma vez que permitiu a familiarização com as técnicas de síntese e caracterização que seriam usadas no trabalho principal do mestrado.

Trata-se da preparação de nanopartículas de maguemita, funcionalizadas com glicina, utilizando um procedimento de baixo custo e ambientalmente correto, como uma via alternativa para as rotas típicas para a elaboração de nanomateriais magnéticos funcionalizados com polímeros aminados, para remoção magnética de cobre em água contaminada. De maneira resumida – o anexo D traz o referido artigo com os detalhes experimentais e discussão científica –nanopartículas magnéticas (maguemita) de ~12 nm foram sintetizadas por coprecipitação em meio alcalino. Foi observado que a glicina era melhor adsorvida em pH ~ 6 e que a saturação da adsorção de moléculas na superfície do óxido ocorreu na forma de monocamada, em uma razão de 10 % em massa de glicina/nanopartículas magnética. Especificamente, os grupos carboxilato da glicina coordenam fortemente os íons férricos da superfície da nanopartículas, enquanto os grupos amina ficam voltados para a solução formando um recobrimento reforçado. Foi observado que as nanopartículas modificadas apresentavam forte afinidade pelos íons Cu^{2+}, devido à interação eletrostática e complexação dos grupos amina com esse metal. A cinética de adsorção se mostrou dependente do pH do meio, seguindo um mecanismo de pseudo-segunda ordem. O equilíbrio de adsorção para o cobre seguiu uma isoterma de Langmuir com alta capacidade de adsorção.

Mais especificamente, os resultados sugerem que essas nanopartículas modificadas são altamente efetivas e de baixo custo, como nanosorbentes, para

remoção de cobre – podendo esse procedimento ser estendido a outros metais com afinidade aos grupos amina – em amostras de água, em comparação aos métodos industriais de purificação existentes. Além disso, esses nanosorbentes magnéticos podem ser facilmente separados da solução com a ajuda de um campo magnético externo e depois reutilizado, após reciclagem – remoção dos íons adsorvidos.

2. Conclusões e perspectivas

Por meio da precipitação homogênea com ureia, nanopartículas de quitosana com cerca de 100 nm, incrustradas de nanopartículas magnéticas de óxido de ferro (magnetita/maguemita) de ~5 nm foram sintetizadas. Uma das vantagens do procedimento para a síntese da quitosana magnética aqui apresentado reside no fato de que um fármaco selecionado (triptofano) pôde ser incorporado de maneira eficiente durante o procedimento de síntese do nanocompósito, gerando um procedimento de uma única etapa. A liberação do triptofano se mostrou dependente do tempo e influenciada pelo pH do meio sendo, nesse caso, modulada pela difusão do fármaco originada pelo entumescimento e/ou dissolução do polímero, além da dessorção superficial.

Devido à natureza química da quitosana e dos óxidos magnéticos, a incorporação poderia ser estendida a outros fármacos diferentes do triptofano e, de acordo com as características magnéticas, esse compósito poderia ser facilmente manipulado por um campo magnético externo para ser conduzido e/ou concentrado em determinada região alvo, aumentando a eficiência do sistema de liberação controlada. Além disso, sendo a decomposição e o entumescimento do polímero dependentes da temperatura, o aquecimento via aplicação de um campo alternado (magneto-hipertermia) poderia ser utilizado para modular a liberação do fármaco.

Nesse sentido, a rota de síntese apresentada nesse trabalho tem grande potencial como alta eficiência, baixo custo e a utilização de reagentes menos agressivos ao meio ambiente para a síntese materiais estímulo-responsíveis para aplicações no campo de sistemas de liberação controlada e sustentável de fármacos.

REFERÊNCIAS

Não contidas no artigo científico

REFERÊNCIAS

1. Anirudhan TS, Gopal SS, Sandeep S. Synthesis and characterization of montmorillonite/N-(carboxyacyl) chitosan coated magnetic particle nanocomposites for controlled delivery of paracetamol. Appl Clay Sci. 2014 Feb;88-89:151-8. PubMed PMID: WOS:000331773400020. English

2. Alonso MJ. Nanomedicines for overcoming biological barriers. Biomed Pharmacother. 2004 Apr;58(3):168-72. PubMed PMID: WOS:000221409100005. English.

3. Agnihotri SA, Mallikarjuna NN, Aminabhavi TM. Recent advances on chitosan-based micro- and nanoparticles in drug delivery. J Control Release. 2004 Nov 5;100(1):5-28. PubMed PMID: WOS:000225177900002. English.

4. Azevedo MMM.Nanoesferas e a liberação controlada de fármacos [monografia]. Campinas: Universidade de Campinas – UNICAMP; 2002.

5. Bae KH, Park M, Do MJ, Lee N, Ryu JH, Kim GW, et al. Chitosan Oligosaccharide-Stabilized Ferrimagnetic Iron Oxide Nanocubes for Magnetically Modulated Cancer Hyperthermia. Acs Nano. 2012 Jun;6(6):5266-73. PubMed PMID: WOS:000305661300078. English.

6. Babes L, Denizot B, Tanguy G, Le Jeune JJ, Jallet P. Synthesis of iron oxide nanoparticles used as MRI contrast agents: A parametric study. J Colloid Interf Sci. 1999 Apr 15;212(2):474-82. PubMed PMID: WOS:000079500500033. English.

7. Berry CC, Curtis ASG. Functionalisation of magnetic nanoparticles for applications in biomedicine. J Phys D Appl Phys. 2003 Jul 7;36(13):R198-R206. PubMed PMID: WOS:000185360900006. English.

8. Bush ES, Hazelwood L. *In* Brunton LL, Chabner BA, Knollmann B. As bases farmacológicas da terapêutica de Goodman & Gilman. 12ª ed. Porto Alegre: AMGH; 2012. p. 335-361.

9. Brugnerotto J, Desbrières J, Roberts G, Rinaudo M. Charccterization of chitosan by steric exclusion chromatograph. Pol. 2001 Dec;42(25):9921-9927.

10. Carvalho CC, Chorilli M, Gremião MPD. Plataformas Bio (muco) adesivas poliméricas baseadas em nanotecnologia para liberação controlada de fármacos – propriedades metodologias e aplicações. Pol. 2014, 24(2):203-213.

11. Coelho JF, Ferreira PC, Alves P, Cordeiro R, Fonseca AC, Gois JR, et al. Drug delivery systems: Advanced technologies potentially applicable in personalized treatments. The EPMA journal. 2010 Mar;1(1):164-209. PubMed PMID: 23199049. Pubmed Central PMCID: 3405312.

12. Comai S, Bertazzo A, Bailoni L, Zancato M, Costa CVL, Allegri G. The content of proteic and nonproteic (free and protein-bound) tryptophan in quinoa and cereal flours. Food Chem. 2007;100(4):1350-5. PubMed PMID: WOS:000241000300009. English.

13. De Geest BG, De Koker S, Sukhorukov GB, Kreft O, Parak WJ, Skirtach AG, et al. Polyelectrolyte microcapsules for biomedical applications. Soft Matter. 2009;5(2):282-91. PubMed PMID: WOS:000262956100003. English.

14. De Jong WH, Borm PJ. Drug delivery and nanoparticles:applications and hazards. International journal of nanomedicine. 2008;3(2):133-49. PubMed PMID: 18686775. Pubmed Central PMCID: 2527668.

15. delMonte F, Morales MP, Levy D, Fernandez A, Ocana M, Roig A, et al. Formation of gamma-Fe2O3 isolated nanoparticles in a silica matrix. Langmuir. 1997 Jul 9;13(14):3627-34. PubMed PMID: WOS:A1997XJ92500007. English.

16. Dobson J. Magnetic micro- and nano-particle-based targeting for drug and gene delivery. Nanomedicine. 2006 Jun;1(1):31-7. PubMed PMID: WOS:000243784100013. English.

17. Gupta AK, Gupta M. Synthesis and surface engineering of iron oxide nanoparticles for biomedical applications. Biomaterials. 2005 Jun;26(18):3995-4021. PubMed PMID: WOS:000227143800024. English

18. Johannsen M, Thiesen B, Wust P, Jordan A. Magnetic nanoparticle hyperthermia for prostate cancer. Int J Hyperther. 2010;26(8):790-5. PubMed PMID: WOS:000283738500006. English.

19. Kapczinski F, Busnello JV, Abreu MR, Carrao AD. Aspectos da fisiologia do triptofano. Rev. Psiq. Clin. 1998, 25(4):158-165.

20. Kopp AF, Laniado M, Dammann F, Stern W, Gronewaller E, Balzer T, et al. MR imaging of the liver with resovist: Safety, efficacy, and pharmacodynamic properties. Radiology. 1997 Sep;204(3):749-56. PubMed PMID: WOS:A1997XR60200026. English.

21. Laurent S, Forge D, Port M, Roch A, Robic C, Elst LV, et al. Magnetic iron oxide nanoparticles: Synthesis, stabilization, vectorization, physicochemical

characterizations, and biological applications. Chem Rev. 2008 Jun;108(6):2064-110. PubMed PMID: WOS:000256738100009. English

22. Lin Y, Sun X, Yuan Q, Yan Y. Engineering Bacterial Phenylalanine 4-Hydroxylase for Microbial Synthesis of Human Neurotransmitter Precursor 5-Hydroxytryptophan. ACS synthetic biology. 2014 Jun 30. PubMed PMID: 24936877.

23. Lu ZH, Prouty MD, Guo ZH, Golub VO, Kumar CSSR, Lvov YM. Magnetic switch of permeability for polyelectrolyte microcapsules embedded with Co@Au nanoparticles. Langmuir. 2005 Mar 1;21(5):2042-50. PubMed PMID: WOS:000227193500059. English.

24. Madihally SV, Matthew HW. Porous chitosan scaffolds for tissue engineering. Biomaterials. 1999 Jun;20(12):1133-42. PubMed PMID: 10382829.

25. Majumdar APN. Tryptophan Requirement for Protein-Synthesis - a Review. Nutr Rep Int. 1982;26(3):509-22. PubMed PMID: WOS:A1982PF72600023. English

26. Neuberger T, Schopf B, Hofmann H, Hofmann M, von Rechenberg B. Superparamagnetic nanoparticles for biomedical applications: Possibilities and limitations of a new drug delivery system. J Magn Magn Mater. 2005 May 1;293(1):483-96. PubMed PMID: WOS:000229661400074. English.

27. Pankhurst QA, Thanh NTK, Jones SK, Dobson J. Progress in applications of magnetic nanoparticles in biomedicine. J Phys D Appl Phys. 2009 Nov 21;42(22). PubMed PMID: WOS:000271519000005. English.

28. Pankhurst QA, Connolly J, Jones SK, Dobson J. Applications of magnetic nanoparticles in biomedicine. J Phys D Appl Phys. 2003 Jul 7;36(13):R167-R81. PubMed PMID: WOS:000185360900004. English.

29. Petrovic DM, Hesp BH, Broos J. Emitting state of 5-hydroxyindole, 5-hydroxytryptophan, and 5-hydroxytryptophan incorporated in proteins. The journal of physical chemistry B. 2013 Sep 19;117(37):10792-7. PubMed PMID: 24020960.

30. Pezzini BR, Silva MAS, Ferraz HG. Formas farmacêuticas sólidas orais de liberação prolongada: sistemas monolíticos e multiparticulados. Rev. Bras. Cienc. Farm. 2007; Out;43(4):491-502.

31. Picart C, Schneider A, Etienne O, Mutterer J, Schaaf P, Egles C, et al. Controlled degradability of polysaccharide multilayer films in vitro and in vivo. Adv Funct Mater. 2005 Nov;15(11):1771-80. PubMed PMID: WOS:000233279500005. English.

32. Reddy LH, Arias JL, Nicolas J, Couvreur P. Magnetic Nanoparticles: Design and Characterization, Toxicity and Biocompatibility, Pharmaceutical and Biomedical Applications. Chem Rev. 2012 Nov;112(11):5818-78. PubMed PMID: WOS:000311239600008. English.

33. Roca AG, Costo R, Rebolledo AF, Veintemillas-Verdaguer S, Tartaj P, Gonzalez-Carreno T, et al. Progress in the preparation of magnetic nanoparticles for applications in biomedicine. J Phys D Appl Phys. 2009 Nov 21;42(22). PubMed PMID: WOS:000271519000006. English

34. Severino P, Santana MHA, Malmonge SM, Souto EB. Polímeros usados como sistema de transporte de princípios ativos. Polimeros. 2011;Set;21(5):361-368

35. Sieguel RA, Rathbone MJ. Overview of controlled release mechanisms. In: J. Siepmann et al. Fundamentals and applications of controlled release drug delivery, advances in delivery science and technology. Minnesota: Harvard; 2012. p. 19 – 43.

36. Shchukin DG, Gorin DA, Moehwald H. Ultrasonically induced opening of polyelectrolyte microcontainers. Langmuir. 2006 Aug 15;22(17):7400-4. PubMed PMID: WOS:000239596300050. English.

37. Schaffazick SR, Gutterres SS, Freitas LP. Caracterização e estabilidade fisicoquímica de sistema poliméricos nanoparticulados para administração de fármacos. Quimica Nova 2003;Set;26(5): 726-737

38. Skirtach AG, Antipov AA, Shchukin DG, Sukhorukov GB. Remote activation of capsules containing Ag nanoparticles and IR dye by laser light. Langmuir. 2004 Aug 17;20(17):6988-92. PubMed PMID: WOS:000223276400007. English

39. Shi JJ, Votruba AR, Farokhzad OC, Langer R. Nanotechnology in Drug Delivery and Tissue Engineering: From Discovery to Applications. Nano Lett. 2010 Sep;10(9):3223-30. PubMed PMID: WOS:000281498200001. English.

40. Soppimath KS, Aminabhavi TM, Kulkarni AR, Rudzinski WE. Biodegradable polymeric nanoparticles as drug delivery devices. J Control Release. 2001 Jan 29;70(1-2):1-20. PubMed PMID: WOS:000166774600001. English.

41. Sun C, Lee JSH, Zhang MQ. Magnetic nanoparticles in MR imaging and drug delivery. Adv Drug Deliver Rev. 2008 Aug 17;60(11):1252-65. PubMed PMID: WOS:000258313900004. English.

42. Tran PHL, Tran TTD, Park JB, Lee BJ. Controlled Release Systems Containing Solid Dispersions: Strategies and Mechanisms. Pharm Res-Dordr. 2011 Oct;28(10):2353-78. PubMed PMID: WOS:000294811700001. English.

43. Tunna IJ, Patel BA. Analysis of 5-hydroxytryptophan in the presence of excipients from dietary capsules: comparison between cyclic voltammetry and UV visible spectroscopy. Anal Methods-Uk. 2013;5(10):2523-8. PubMed PMID: WOS:000318314700013. English.

44. Uria VJG, Garcia MRI, Pacheco FP, Viloria A, Higuera T, Laborda A, et al . Estudio experimental sobre quimioterapia focalizada em riñón mediante arpón magnético y administración intravenosa de nanopartículas ferrocarbonosas. Arch. Esp. Urol. 2007;May; 60(1):5-14.

45. Verde EL, Landi GT, Gomes JA, Sousa MH, Bakuzis AF. Magnetic hyperthermia investigation of cobalt ferrite nanoparticles: Comparison between experiment, linear response theory, and dynamic hysteresis simulations. J Appl Phys. 2012 Jun 15;111(12). PubMed PMID: WOS:000305832100076. English.

46. Verde EL, Landi GT, Carriao MS, Drummond AL, Gomes JA, Vieira ED, et al. Field dependent transition to the non-linear regime in magnetic hyperthermia experiments: Comparison between maghemite, copper, zinc, nickel and cobalt ferrite nanoparticles of similar sizes. Aip Adv. 2012 Sep;2(3). PubMed PMID: WOS:000309388800020. English.

47. Villanova,J.C .O; Oréfice, R.L.; Cunha, A.S.. Aplicações Farmacêuticas de Polímeros. Polímeros.2010; Mar;20(1):51-64

48. You JO, Almeda D, Ye GJ, Auguste DT. Bioresponsive matrices in drug delivery. Journal of biological engineering. 2010;4:15. PubMed PMID: 21114841. Pubmed Central PMCID: 3002303.

49. Ziolo RF, Giannelis EP, Weinstein BA, O'Horo MP, Ganguly BN, Mehrotra V,et al. Matrix-mediated synthesis of nanocrystalline γ-Fe2O3: a new optically transparent magnetic material. 1992 Jul 257:219-222.

ANEXO A

Normas específicas para publicação no periódico

Journal of Magnetism and Magnetic Materials

JOURNAL OF MAGNETISM AND MAGNETIC MATERIALS

AUTHOR INFORMATION PACK

TABLE OF CONTENTS

ISSN: 0304-8853

DESCRIPTION

The *Journal of Magnetism and Magnetic Materials* provides an important forum for the disclosure and discussion of original contributions covering the whole spectrum of topics, from basic **magnetism** to the technology and applications of **magnetic materials** and **magnetic recording**. The journal encourages greater interaction between the basic and applied subdisciplines of magnetism with short but comprehensive review articles, a rapid publication channel with "Letters to the Editor", in addition to full-length contributions. The section on *Information Storage: Basic and Applied* contains articles on all topics in magnetic recording media and processes.

Benefits to authors
We also provide many author benefits, such as free PDFs, a liberal copyright policy, special discounts on Elsevier publications and much more. Please click here for more information on our author services.

Please see our Guide for Authors for information on article submission. If you require any further information or help, please visit our support pages: http://support.elsevier.com

AUDIENCE

Solid state physicists, materials scientists.

IMPACT FACTOR

2012: 1.826 © Thomson Reuters Journal Citation Reports 2013

ABSTRACTING AND INDEXING

Current Contents/Physics, Chemical, & Earth Sciences
Metals Abstracts
EI Compendex Plus
Engineering Index
INSPEC
Scopus

EDITORIAL BOARD

GUIDE FOR AUTHORS

Your Paper Your Way
ypyw-gfa-banner.gifyour paper your way

BEFORE YOU BEGIN

Ethics in publishing

For information on Ethics in publishing and Ethical guidelines for journal publication see http://www.elsevier.com/publishingethics and http://www.elsevier.com/journal-authors/ethics.

Conflict of interest

All authors are requested to disclose any actual or potential conflict of interest including any financial, personal or other relationships with other people or organizations within three years of beginning the submitted work that could inappropriately influence, or be perceived to influence, their work. See also http://www.elsevier.com/conflictsofinterest. Further information and an example of a Conflict of Interest form can be found at: http://help.elsevier.com/app/answers/detail/a_id/286/p/7923.

Submission declaration

Submission of an article implies that the work described has not been published previously (except in the form of an abstract or as part of a published lecture or academic thesis or as an electronic preprint, see http://www.elsevier.com/postingpolicy), that it is not under consideration for publication elsewhere, that its publication is approved by all authors and tacitly or explicitly by the responsible authorities where the work was carried out, and that, if accepted, it will not be published elsewhere including electronically in the same form, in English or in any other language, without the written consent of the copyright-holder.

Changes to authorship

This policy concerns the addition, deletion, or rearrangement of author names in the authorship of accepted manuscripts:
Before the accepted manuscript is published in an online issue: Requests to add or remove an author, or to rearrange the author names, must be sent to the Journal Manager from the corresponding author of the accepted manuscript and must include: (a) the reason the name should be added or removed, or the author names rearranged and (b) written confirmation (e-mail, fax, letter) from all authors that they agree with the addition, removal or rearrangement. In the case of addition or removal of authors, this includes confirmation from the author being added or removed. Requests that are not sent by the corresponding author will be forwarded by the Journal Manager to the corresponding author, who must follow the procedure as described above. Note that: (1) Journal Managers will inform the Journal Editors of any such requests and (2) publication of the accepted manuscript in an online issue is suspended until authorship has been agreed.
After the accepted manuscript is published in an online issue: Any requests to add, delete, or rearrange author names in an article published in an online issue will follow the same policies as noted above and result in a corrigendum.

Copyright

This journal offers authors a choice in publishing their research: Open access and Subscription.

For subscription articles
Upon acceptance of an article, authors will be asked to complete a 'Journal Publishing Agreement' (for more information on this and copyright, see http://www.elsevier.com/copyright). An e-mail will be sent to the corresponding author confirming receipt of the manuscript together with a 'Journal Publishing Agreement' form or a link to the online version of this agreement.
Subscribers may reproduce tables of contents or prepare lists of articles including abstracts for internal circulation within their institutions. Permission of the Publisher is required for resale or distribution outside the institution and for all other derivative works, including compilations and translations (please consult http://www.elsevier.com/permissions). If excerpts from other copyrighted works are included, the author(s) must obtain written permission from the copyright owners and credit the source(s) in the article. Elsevier has preprinted forms for use by authors in these cases: please consult http://www.elsevier.com/permissions.

For open access articles

Upon acceptance of an article, authors will be asked to complete an 'Exclusive License Agreement' (for more information see http://www.elsevier.com/OAauthoragreement). Permitted reuse of open access articles is determined by the author's choice of user license (see http://www.elsevier.com/openaccesslicenses).

Retained author rights
As an author you (or your employer or institution) retain certain rights. For more information on author rights for:
Subscription articles please see http://www.elsevier.com/journal-authors/author-rights-and-responsibilities.
Open access articles please see http://www.elsevier.com/OAauthoragreement.

Role of the funding source
You are requested to identify who provided financial support for the conduct of the research and/or preparation of the article and to briefly describe the role of the sponsor(s), if any, in study design; in the collection, analysis and interpretation of data; in the writing of the report; and in the decision to submit the article for publication. If the funding source(s) had no such involvement then this should be stated.

Funding body agreements and policies
Elsevier has established agreements and developed policies to allow authors whose articles appear in journals published by Elsevier, to comply with potential manuscript archiving requirements as specified as conditions of their grant awards. To learn more about existing agreements and policies please visit http://www.elsevier.com/fundingbodies.

Open access
This journal offers authors a choice in publishing their research:

Open access
• Articles are freely available to both subscribers and the wider public with permitted reuse
• An open access publication fee is payable by authors or their research funder
Subscription
• Articles are made available to subscribers as well as developing countries and patient groups through our access programs (http://www.elsevier.com/access)
• No open access publication fee

All articles published open access will be immediately and permanently free for everyone to read and download. Permitted reuse is defined by your choice of one of the following Creative Commons user licenses:
Creative Commons Attribution (CC BY): lets others distribute and copy the article, to create extracts, abstracts, and other revised versions, adaptations or derivative works of or from an article (such as a translation), to include in a collective work (such as an anthology), to text or data mine the article, even for commercial purposes, as long as they credit the author(s), do not represent the author as endorsing their adaptation of the article, and do not modify the article in such a way as to damage the author's honor or reputation.
Creative Commons Attribution-NonCommercial-ShareAlike (CC BY-NC-SA): for non-commercial purposes, lets others distribute and copy the article, to create extracts, abstracts and other revised versions, adaptations or derivative works of or from an article (such as a translation), to include in a collective work (such as an anthology), to text and data mine the article, as long as they credit the author(s), do not represent the author as endorsing their adaptation of the article, do not modify the article in such a way as to damage the author's honor or reputation, and license their new adaptations or creations under identical terms (CC BY-NC-SA).
Creative Commons Attribution-NonCommercial-NoDerivs (CC BY-NC-ND): for non-commercial purposes, lets others distribute and copy the article, and to include in a collective work (such as an anthology), as long as they credit the author(s) and provided they do not alter or modify the article.

To provide open access, this journal has a publication fee which needs to be met by the authors or their research funders for each article published open access.
Your publication choice will have no effect on the peer review process or acceptance of submitted articles.

The publication fee for this journal is **$2200**, excluding taxes. Learn more about Elsevier's pricing policy: http://www.elsevier.com/openaccesspricing.

Language (usage and editing services)

Please write your text in good English (American or British usage is accepted, but not a mixture of these). Authors who feel their English language manuscript may require editing to eliminate possible grammatical or spelling errors and to conform to correct scientific English may wish to use the English Language Editing service available from Elsevier's WebShop (http://webshop.elsevier.com/languageediting/) or visit our customer support site (http://support.elsevier.com) for more information.

Submission

Submission to this journal proceeds totally online and you will be guided stepwise through the creation and uploading of your files. The system automatically converts source files to a single PDF file of the article, which is used in the peer-review process. Please note that even though manuscript source files are converted to PDF files at submission for the review process, these source files are needed for further processing after acceptance. All correspondence, including notification of the Editor's decision and requests for revision, takes place by e-mail removing the need for a paper trail.

PREPARATION

NEW SUBMISSIONS

Submission to this journal proceeds totally online and you will be guided stepwise through the creation and uploading of your files. The system automatically converts your files to a single PDF file, which is used in the peer-review process.
As part of the Your Paper Your Way service, you may choose to submit your manuscript as a single file to be used in the refereeing process. This can be a PDF file or a Word document, in any format or lay-out that can be used by referees to evaluate your manuscript. It should contain high enough quality figures for refereeing. If you prefer to do so, you may still provide all or some of the source files at the initial submission. Please note that individual figure files larger than 10 MB must be uploaded separately.

References

There are no strict requirements on reference formatting at submission. References can be in any style or format as long as the style is consistent. Where applicable, author(s) name(s), journal title/book title, chapter title/article title, year of publication, volume number/book chapter and the pagination must be present. Use of DOI is highly encouraged. The reference style used by the journal will be applied to the accepted article by Elsevier at the proof stage. Note that missing data will be highlighted at proof stage for the author to correct.

Formatting requirements

There are no strict formatting requirements but all manuscripts must contain the essential elements needed to convey your manuscript, for example Abstract, Keywords, Introduction, Materials and Methods, Results, Conclusions, Artwork and Tables with Captions.
If your article includes any Videos and/or other Supplementary material, this should be included in your initial submission for peer review purposes.
Divide the article into clearly defined sections.

Figures and tables embedded in text

Please ensure the figures and the tables included in the single file are placed next to the relevant text in the manuscript, rather than at the bottom or the top of the file.

REVISED SUBMISSIONS

Use of word processing software

Regardless of the file format of the original submission, at revision you must provide us with an editable file of the entire article. Keep the layout of the text as simple as possible. Most formatting codes will be removed and replaced on processing the article. The electronic text should be prepared in a way very similar to that of conventional manuscripts (see also the Guide to Publishing with Elsevier: http://www.elsevier.com/guidepublication). See also the section on Electronic artwork.
To avoid unnecessary errors you are strongly advised to use the 'spell-check' and 'grammar-check' functions of your word processor.

LaTeX

You are recommended to use the Elsevier article class *elsarticle.cls* (http://www.ctan.org/tex-archive/macros/latex/contrib/elsarticle) to prepare your manuscript and BibTeX (http://www.bibtex.org) to generate your bibliography.
For detailed submission instructions, templates and other information on LaTeX, see http://www.elsevier.com/latex.

Article structure

Subdivision - numbered sections
Divide your article into clearly defined and numbered sections. Subsections should be numbered 1.1 (then 1.1.1, 1.1.2, ...), 1.2, etc. (the abstract is not included in section numbering). Use this numbering also for internal cross-referencing: do not just refer to 'the text'. Any subsection may be given a brief heading. Each heading should appear on its own separate line.

Introduction
State the objectives of the work and provide an adequate background, avoiding a detailed literature survey or a summary of the results.

Material and methods
Provide sufficient detail to allow the work to be reproduced. Methods already published should be indicated by a reference: only relevant modifications should be described.

Theory/calculation
A Theory section should extend, not repeat, the background to the article already dealt with in the Introduction and lay the foundation for further work. In contrast, a Calculation section represents a practical development from a theoretical basis.

Results
Results should be clear and concise.

Discussion
This should explore the significance of the results of the work, not repeat them. A combined Results and Discussion section is often appropriate. Avoid extensive citations and discussion of published literature.

Conclusions
The main conclusions of the study may be presented in a short Conclusions section, which may stand alone or form a subsection of a Discussion or Results and Discussion section.

Appendices
If there is more than one appendix, they should be identified as A, B, etc. Formulae and equations in appendices should be given separate numbering: Eq. (A.1), Eq. (A.2), etc.; in a subsequent appendix, Eq. (B.1) and so on. Similarly for tables and figures: Table A.1; Fig. A.1, etc.

Essential title page information

• ***Title.*** Concise and informative. Titles are often used in information-retrieval systems. Avoid abbreviations and formulae where possible.
• ***Author names and affiliations.*** Where the family name may be ambiguous (e.g., a double name), please indicate this clearly. Present the authors' affiliation addresses (where the actual work was done) below the names. Indicate all affiliations with a lower-case superscript letter immediately after the author's name and in front of the appropriate address. Provide the full postal address of each affiliation, including the country name and, if available, the e-mail address of each author.
• ***Corresponding author.*** Clearly indicate who will handle correspondence at all stages of refereeing and publication, also post-publication. **Ensure that phone numbers (with country and area code) are provided in addition to the e-mail address and the complete postal address. Contact details must be kept up to date by the corresponding author.**
• ***Present/permanent address.*** If an author has moved since the work described in the article was done, or was visiting at the time, a 'Present address' (or 'Permanent address') may be indicated as a footnote to that author's name. The address at which the author actually did the work must be retained as the main, affiliation address. Superscript Arabic numerals are used for such footnotes.

Abstract
A concise and factual abstract is required. The abstract should state briefly the purpose of the research, the principal results and major conclusions. An abstract is often presented separately from the article, so it must be able to stand alone. For this reason, References should be avoided, but if essential, then cite the author(s) and year(s). Also, non-standard or uncommon abbreviations should be avoided, but if essential they must be defined at their first mention in the abstract itself.

Highlights
Highlights are mandatory for this journal. They consist of a short collection of bullet points that convey the core findings of the article and should be submitted in a separate file in the online submission system. Please use 'Highlights' in the file name and include 3 to 5 bullet points (maximum 85 characters, including spaces, per bullet point). See http://www.elsevier.com/highlights for examples.

Keywords
Immediately after the abstract, provide a maximum of 6 keywords, using American spelling and avoiding general and plural terms and multiple concepts (avoid, for example, 'and', 'of'). Be sparing with abbreviations: only abbreviations firmly established in the field may be eligible. These keywords will be used for indexing purposes.

Abbreviations
Define abbreviations that are not standard in this field in a footnote to be placed on the first page of the article. Such abbreviations that are unavoidable in the abstract must be defined at their first mention there, as well as in the footnote. Ensure consistency of abbreviations throughout the article.

Acknowledgements
Collate acknowledgements in a separate section at the end of the article before the references and do not, therefore, include them on the title page, as a footnote to the title or otherwise. List here those individuals who provided help during the research (e.g., providing language help, writing assistance or proof reading the article, etc.).

Math formulae
Present simple formulae in the line of normal text where possible and use the solidus (/) instead of a horizontal line for small fractional terms, e.g., X/Y. In principle, variables are to be presented in italics. Powers of e are often more conveniently denoted by exp. Number consecutively any equations that have to be displayed separately from the text (if referred to explicitly in the text).

Footnotes
Footnotes should be used sparingly. Number them consecutively throughout the article. Many wordprocessors build footnotes into the text, and this feature may be used. Should this not be the case, indicate the position of footnotes in the text and present the footnotes themselves separately at the end of the article. Do not include footnotes in the Reference list.

Table footnotes

Indicate each footnote in a table with a superscript lowercase letter.

Artwork
Electronic artwork

General points

• Make sure you use uniform lettering and sizing of your original artwork.
• Preferred fonts: Arial (or Helvetica), Times New Roman (or Times), Symbol, Courier.
• Number the illustrations according to their sequence in the text.
• Use a logical naming convention for your artwork files.
• Indicate per figure if it is a single, 1.5 or 2-column fitting image.
• For Word submissions only, you may still provide figures and their captions, and tables within a single file at the revision stage.
• Please note that individual figure files larger than 10 MB must be provided in separate source files.

A detailed guide on electronic artwork is available on our website:
http://www.elsevier.com/artworkinstructions.
You are urged to visit this site; some excerpts from the detailed information are given here.

Formats

Regardless of the application used, when your electronic artwork is finalized, please 'save as' or convert the images to one of the following formats (note the resolution requirements for line drawings, halftones, and line/halftone combinations given below):
EPS (or PDF): Vector drawings. Embed the font or save the text as 'graphics'.

TIFF (or JPG): Color or grayscale photographs (halftones): always use a minimum of 300 dpi.
TIFF (or JPG): Bitmapped line drawings: use a minimum of 1000 dpi.
TIFF (or JPG): Combinations bitmapped line/half-tone (color or grayscale): a minimum of 500 dpi is required.
Please do not:
• Supply files that are optimized for screen use (e.g., GIF, BMP, PICT, WPG); the resolution is too low.
• Supply files that are too low in resolution.
• Submit graphics that are disproportionately large for the content.

Non-electronic artwork
Provide all illustrations as high-quality printouts, suitable for reproduction (which may include reduction) without retouching. Number illustrations consecutively in the order in which they are referred to in the text. They should accompany the manuscript, but should not be included within the text. Clearly mark all illustrations on the back (or - in case of line drawings - on the lower front side) with the figure number and the author's name and, in cases of ambiguity, the correct orientation. Mark the appropriate position of a figure in the article.

Color artwork
Please make sure that artwork files are in an acceptable format (TIFF (or JPEG), EPS (or PDF), or MS Office files) and with the correct resolution. If, together with your accepted article, you submit usable color figures then Elsevier will ensure, at no additional charge, that these figures will appear in color on the Web (e.g., ScienceDirect and other sites) regardless of whether or not these illustrations are reproduced in color in the printed version. **For color reproduction in print, you will receive information regarding the costs from Elsevier after receipt of your accepted article**. Please indicate your preference for color: in print or on the Web only. For further information on the preparation of electronic artwork, please see http://www.elsevier.com/artworkinstructions.
Please note: Because of technical complications which can arise by converting color figures to 'gray scale' (for the printed version should you not opt for color in print) please submit in addition usable black and white versions of all the color illustrations.

Figure captions
Ensure that each illustration has a caption. A caption should comprise a brief title (**not** on the figure itself) and a description of the illustration. Keep text in the illustrations themselves to a minimum but explain all symbols and abbreviations used.

Tables
Number tables consecutively in accordance with their appearance in the text. Place footnotes to tables below the table body and indicate them with superscript lowercase letters. Avoid vertical rules. Be sparing in the use of tables and ensure that the data presented in tables do not duplicate results described elsewhere in the article.

References
Citation in text
Please ensure that every reference cited in the text is also present in the reference list (and vice versa). Any references cited in the abstract must be given in full. Unpublished results and personal communications are not recommended in the reference list, but may be mentioned in the text. If these references are included in the reference list they should follow the standard reference style of the journal and should include a substitution of the publication date with either 'Unpublished results' or 'Personal communication'. Citation of a reference as 'in press' implies that the item has been accepted for publication.

Reference links
Increased discoverability of research and high quality peer review are ensured by online links to the sources cited. In order to allow us to create links to abstracting and indexing services, such as Scopus, CrossRef and PubMed, please ensure that data provided in the references are correct. Please note that incorrect surnames, journal/book titles, publication year and pagination may prevent link creation. When copying references, please be careful as they may already contain errors. Use of the DOI is encouraged.

Web references
As a minimum, the full URL should be given and the date when the reference was last accessed. Any further information, if known (DOI, author names, dates, reference to a source publication, etc.), should also be given. Web references can be listed separately (e.g., after the reference list) under a different heading if desired, or can be included in the reference list.

References in a special issue
Please ensure that the words 'this issue' are added to any references in the list (and any citations in the text) to other articles in the same Special Issue.

Reference management software
This journal has standard templates available in key reference management packages EndNote (http://www.endnote.com/support/enstyles.asp) and Reference Manager (http://refman.com/support/rmstyles.asp). Using plug-ins to wordprocessing packages, authors only need to select the appropriate journal template when preparing their article and the list of references and citations to these will be formatted according to the journal style which is described below.

Reference formatting
There are no strict requirements on reference formatting at submission. References can be in any style or format as long as the style is consistent. Where applicable, author(s) name(s), journal title/book title, chapter title/article title, year of publication, volume number/book chapter and the pagination must be present. Use of DOI is highly encouraged. The reference style used by the journal will be applied to the accepted article by Elsevier at the proof stage. Note that missing data will be highlighted at proof stage for the author to correct. If you do wish to format the references yourself they should be arranged according to the following examples:

Reference style
Text: Indicate references by number(s) in square brackets in line with the text. The actual authors can be referred to, but the reference number(s) must always be given.
Example: '..... as demonstrated [3,6]. Barnaby and Jones [8] obtained a different result ....'
List: Number the references (numbers in square brackets) in the list in the order in which they appear in the text.
Examples:
Reference to a journal publication:
[1] J. van der Geer, J.A.J. Hanraads, R.A. Lupton, The art of writing a scientific article, J. Sci. Commun. 163 (2010) 51–59.
Reference to a book:
[2] W. Strunk Jr., E.B. White, The Elements of Style, fourth ed., Longman, New York, 2000.
Reference to a chapter in an edited book:
[3] G.R. Mettam, L.B. Adams, How to prepare an electronic version of your article, in: B.S. Jones, R.Z. Smith (Eds.), Introduction to the Electronic Age, E-Publishing Inc., New York, 2009, pp. 281–304.

Journal abbreviations source
Journal names should be abbreviated according to the List of Title Word Abbreviations: http://www.issn.org/services/online-services/access-to-the-ltwa/.

Video data
Elsevier accepts video material and animation sequences to support and enhance your scientific research. Authors who have video or animation files that they wish to submit with their article are strongly encouraged to include links to these within the body of the article. This can be done in the same way as a figure or table by referring to the video or animation content and noting in the body text where it should be placed. All submitted files should be properly labeled so that they directly relate to the video file's content. In order to ensure that your video or animation material is directly usable, please provide the files in one of our recommended file formats with a preferred maximum size of 50 MB. Video and animation files supplied will be published online in the electronic version of your article in Elsevier Web products, including ScienceDirect: http://www.sciencedirect.com. Please supply 'stills' with your files: you can choose any frame from the video or animation or make a separate image. These will be used instead of standard icons and will personalize the link to your video data. For more detailed instructions please visit our video instruction pages at http://www.elsevier.com/artworkinstructions. Note: since video and animation cannot be embedded in the print version of the journal, please provide text for both the electronic and the print version for the portions of the article that refer to this content.

AudioSlides
The journal encourages authors to create an AudioSlides presentation with their published article. AudioSlides are brief, webinar-style presentations that are shown next to the online article on ScienceDirect. This gives authors the opportunity to summarize their research in their own words and

to help readers understand what the paper is about. More information and examples are available at http://www.elsevier.com/audioslides. Authors of this journal will automatically receive an invitation e-mail to create an AudioSlides presentation after acceptance of their paper.

Supplementary data

Elsevier accepts electronic supplementary material to support and enhance your scientific research. Supplementary files offer the author additional possibilities to publish supporting applications, high-resolution images, background datasets, sound clips and more. Supplementary files supplied will be published online alongside the electronic version of your article in Elsevier Web products, including ScienceDirect: http://www.sciencedirect.com. In order to ensure that your submitted material is directly usable, please provide the data in one of our recommended file formats. Authors should submit the material in electronic format together with the article and supply a concise and descriptive caption for each file. For more detailed instructions please visit our artwork instruction pages at http://www.elsevier.com/artworkinstructions.

Submission checklist

The following list will be useful during the final checking of an article prior to sending it to the journal for review. Please consult this Guide for Authors for further details of any item.

Ensure that the following items are present:

One author has been designated as the corresponding author with contact details:

- E-mail address
- Full postal address
- Telephone

All necessary files have been uploaded, and contain:

- Keywords
- All figure captions
- All tables (including title, description, footnotes)

Further considerations

- Manuscript has been 'spell-checked' and 'grammar-checked'
- All references mentioned in the Reference list are cited in the text, and vice versa
- Permission has been obtained for use of copyrighted material from other sources (including the Web)
- Color figures are clearly marked as being intended for color reproduction on the Web (free of charge) and in print, or to be reproduced in color on the Web (free of charge) and in black-and-white in print
- If only color on the Web is required, black-and-white versions of the figures are also supplied for printing purposes

For any further information please visit our customer support site at http://support.elsevier.com.

AFTER ACCEPTANCE

Use of the Digital Object Identifier

The Digital Object Identifier (DOI) may be used to cite and link to electronic documents. The DOI consists of a unique alpha-numeric character string which is assigned to a document by the publisher upon the initial electronic publication. The assigned DOI never changes. Therefore, it is an ideal medium for citing a document, particularly 'Articles in press' because they have not yet received their full bibliographic information. Example of a correctly given DOI (in URL format; here an article in the journal *Physics Letters B*):

http://dx.doi.org/10.1016/j.physletb.2010.09.059

When you use a DOI to create links to documents on the web, the DOIs are guaranteed never to change.

Online proof correction

Corresponding authors will receive an e-mail with a link to our online proofing system, allowing annotation and correction of proofs online. The environment is similar to MS Word: in addition to editing text, you can also comment on figures/tables and answer questions from the Copy Editor. Web-based proofing provides a faster and less error-prone process by allowing you to directly type your corrections, eliminating the potential introduction of errors.

If preferred, you can still choose to annotate and upload your edits on the PDF version. All instructions for proofing will be given in the e-mail we send to authors, including alternative methods to the online version and PDF.

We will do everything possible to get your article published quickly and accurately - please upload all of your corrections within 48 hours. It is important to ensure that all corrections are sent back to us in one communication. Please check carefully before replying, as inclusion of any subsequent corrections cannot be guaranteed. Proofreading is solely your responsibility. Note that Elsevier may proceed with the publication of your article if no response is received.

Offprints

The corresponding author, at no cost, will be provided with a PDF file of the article via e-mail (the PDF file is a watermarked version of the published article and includes a cover sheet with the journal cover image and a disclaimer outlining the terms and conditions of use). For an extra charge, paper offprints can be ordered via the offprint order form which is sent once the article is accepted for publication. Both corresponding and co-authors may order offprints at any time via Elsevier's WebShop (http://webshop.elsevier.com/myarticleservices/offprints). Authors requiring printed copies of multiple articles may use Elsevier WebShop's 'Create Your Own Book' service to collate multiple articles within a single cover (http://webshop.elsevier.com/myarticleservices/booklets).

Author benefits

Author benefits

*No page charges.*Publishing in the *Journal of Magnetism and Magnetic Materials* is free.*Free offprints.* The corresponding author will receive 25 offprints free of charge. An offprint order form will be supplied by the Publisher for ordering any additional paid offprints.*Discount.* Contributors to Elsevier journals are entitled to a 30% discount on all Elsevier books.

AUTHOR INQUIRIES

For inquiries relating to the submission of articles (including electronic submission) please visit this journal's homepage. For detailed instructions on the preparation of electronic artwork, please visit http://www.elsevier.com/artworkinstructions. Contact details for questions arising after acceptance of an article, especially those relating to proofs, will be provided by the publisher. You can track accepted articles at http://www.elsevier.com/trackarticle. You can also check our Author FAQs at http://www.elsevier.com/authorFAQ and/or contact Customer Support via http://support.elsevier.com.

ANEXO B

Classificação Qualis da Capes para o periódico

Journal of Magnetism and Magnetic Materials

Consulta por Título

ISSN	TÍTULO	ESTRATO	ÁREA DE AVALIAÇÃO	STATUS
0304-8853	Journal of Magnetism and Magnetic Materials	A1	ENGENHARIAS II	Atualizado
0304-8853	Journal of Magnetism and Magnetic Materials	A2	BIODIVERSIDADE	Atualizado
0304-8853	Journal of Magnetism and Magnetic Materials	A2	ENGENHARIAS III	Atualizado
0304-8853	Journal of Magnetism and Magnetic Materials	A2	INTERDISCIPLINAR	Atualizado
0304-8853	Journal of Magnetism and Magnetic Materials	B1	ENGENHARIAS IV	Atualizado
0304-8853	Journal of Magnetism and Magnetic Materials	B1	FARMÁCIA	Atualizado
0304-8853	Journal of Magnetism and Magnetic Materials	B1	GEOCIÊNCIAS	Atualizado
0304-8853	Journal of Magnetism and Magnetic Materials	B1	MEDICINA I	Atualizado
0304-8853	Journal of Magnetism and Magnetic Materials	B1	MEDICINA II	Atualizado
0304-8853	Journal of Magnetism and Magnetic Materials	B2	ASTRONOMIA / FÍSICA	Atualizado
0304-8853	Journal of Magnetism and Magnetic Materials	B2	BIOTECNOLOGIA	Atualizado
0304-8853	Journal of Magnetism and Magnetic Materials	B2	CIÊNCIAS BIOLÓGICAS I	Atualizado
0304-8853	Journal of Magnetism and Magnetic Materials	B2	CIÊNCIAS BIOLÓGICAS II	Atualizado
0304-8853	Journal of Magnetism and Magnetic Materials	B2	CIÊNCIAS BIOLÓGICAS III	Atualizado
0304-8853	Journal of Magnetism and Magnetic Materials	B2	MATEMÁTICA / PROBABILIDADE E	Atualizado
0304-8853	Journal of Magnetism and Magnetic Materials	B2	MATERIAIS	Atualizado
0304-8853	Journal of Magnetism and Magnetic Materials	B2	QUÍMICA	Atualizado
0304-8853	Journal of Magnetism and Magnetic Materials	B3	ECONOMIA	Atualizado

ANEXO C

Comprovante de envio de artigo para o periódico

Journal of Magnetism and Magnetic Materials

Gmail by Google

Marcelo Sousa <mhsqui@gmail.com>

Submission Confirmation

1 mensagem

Urs Hafeli <urs.hafeli@ubc.ca> 20 de junho de 2014 21:16
Para: mhsqui@gmail.com

Dear Marcelo,

Your submission entitled "One-step synthesis of magnetic chitosan for controlled release of tryptophan" has been received by Journal of Magnetism and Magnetic Materials

You may check on the progress of your paper by logging on to the Elsevier Editorial System as an author. The URL is http://ees.elsevier.com/magma/.

Your username is: mhsqui@gmail.com
If you need to retrieve password details, please go to:
http://ees.elsevier.com/magma/automail_query.asp

Your manuscript will be given a reference number once an Editor has been assigned.

Thank you for submitting your work to this journal.

Kind regards,

Elsevier Editorial System
Journal of Magnetism and Magnetic Materials

For further assistance, please visit our customer support site at http://help.elsevier.com/app/answers/list/p/7923. Here you can search for solutions on a range of topics, find answers to frequently asked questions and learn more about EES via interactive tutorials. You will also find our 24/7 support contact details should you need any further assistance from one of our customer support representatives.

ANEXO D

Artigo publicado no periódico *Journal of Hazardous Materials*

Journal of Hazardous Materials 264 (2014) 153–160

Contents lists available at ScienceDirect

Journal of Hazardous Materials

journal homepage: www.elsevier.com/locate/jhazmat

Fabrication of glycine-functionalized maghemite nanoparticles for magnetic removal of copper from wastewater

Natálie C. Feitoza[a], Thamires D. Gonçalves[a], Jéssica J. Mesquita[a], Jucely S. Menegucci[a], Mac-Kedson M.S. Santos[a], Juliano A. Chaker[a], Ricardo B. Cunha[b], Anderson M.M. Medeiros[b], Joel C. Rubim[b], Marcelo H. Sousa[a,*]

[a] Universidade de Brasília, Faculdade de Ceilândia, Centro Metropolitano Conjunto A Lote 1, Ceilândia, DF, CEP 72220-900, Brazil
[b] Universidade de Brasília, Instituto de Química, CP 04478, Brasília, DF, CEP 70919-970, Brazil

HIGHLIGHTS

- Glycine-functionalized magnetic nanoadsorbents are proposed for copper removal.
- Nanoadsorbents present highly efficient removal of copper ions from wastewater.
- Nanoadsorbents are magnetically separable and reusable for removal of copper.
- Synthesis utilizes a cost-effective and environmentally friendly procedure.
- Removal can be extended to other heavy metal ions from wastewater.

ARTICLE INFO

Article history:
Received 4 September 2013
Received in revised form 7 November 2013
Accepted 10 November 2013
Available online 18 November 2013

Keywords:
Magnetic nanoparticles
Glycine-functionalized
Wastewater
Copper adsorption

ABSTRACT

Maghemite nanoparticles (MNPs) were functionalized with glycine, by a cost-effective and environmentally friendly procedure, as an alternative route to typical amine-functionalized polymeric coatings, for highly efficient removal of copper ions from water. MNPs were synthesized by co-precipitation method and adsorption of glycine was investigated as a function of ligand concentration and pH. The efficiency of these functionalized nanoparticles for removal of Cu^{2+} from water has been explored and showed that adsorption is highly dependent of pH and that it occurs either by forming chelate complexes and/or by electrostatic interaction. The adsorption process, which reaches equilibrium in few minutes and fits a pseudo second-order model, follows the Langmuir adsorption model with a very high maximum adsorption capacity for Cu^{2+} of 625 mg/g. Furthermore, these nanoadsorbents can be used as highly efficient separable and reusable materials for removal of toxic metal ions.

1. Introduction

Contamination of water with toxic metal ions is becoming a severe environmental and public health problem. Thus, rising demands for clean and safe water in extremely low levels of heavy metal ions make it greatly important to develop improved technologies for heavy metal ions removal. The conventional methods commonly used for the removal of metals from liquid effluents, such as precipitation and flocculation, have several disadvantageous features such as expensive equipment requirement, continuous replenishment of chemicals, time consuming and easy to produce secondary pollution. Alternative methods, as adsorption, present several advantages on the other techniques for water reuse in terms of the initial cost, simplicity of design, ease of operation, low quantity of residues generated, easy recovery of metals and the possibility to reuse the adsorbent [1]. Recent advances suggest that many of the issues involving water quality could be resolved or greatly ameliorated using nanoparticles (NPs), nanofiltration or other products resulting from the development of nanotechnology [2]. Particularly, nanostructured materials have been investigated due to its high superficial adsorbent area and capability of functionalization with different molecules. Moreover its unique physical and physicochemical properties (structural, electrical, optical, magnetic, etc.) can provide unprecedented opportunities for the adsorption of heavy metals ions in highly efficient and cost-effective approaches. Advantageously, the manipulability of magnetic nanoparticles by an external magnetic field gradient opens up many applications involving the environmental area [3,4]. However, bare magnetic nanoparticles present non-specific adsorbent surface, easily

* Corresponding author. Tel.: +55 61 9206 0946.
E-mail addresses: mhsousa@unb.br, mhsqui@gmail.com (M.H. Sousa).

0304-3894/$ – see front matter © 2013 Elsevier B.V. All rights reserved.
http://dx.doi.org/10.1016/j.jhazmat.2013.11.022

aggregating in aqueous systems so that, for effective application, the stabilization of the nanograins by surface modification is desirable. The performance of these nanosystems depends on the nature of the magnetic core and the coatings, which must be of a non-toxic and adsorptive material. By far, magnetite is the most commonly magnetic core employed in these applications, nevertheless it easily oxidizes to maghemite – a more stable magnetic oxide – in aqueous media. Most of these coatings which have been utilized for separating and removing metal contaminants of water are based on biocompatible polymeric matrixes or long chain molecules [5,6]. Nevertheless, in spite of bringing specificity to the nanograins, the non-magnetic coating decreases the saturation magnetization and increases the particle volume. It is important to consider that smallest particles present highest adsorption capabilities and high magnetizations optimize the magnetic separation. To avoid these constraints, an alternative to polymer coatings is the chemical modification of the magnetic nanoparticle surface by small functional molecules.

In this way, glycine was chosen as it is a short molecule with carboxylate groups, easily adsorbed onto the iron oxide surface, and $-NH_2$ groups at surface that could interact with the bio-environment. In fact, the potential of amine-functionalized magnetic nanoparticles was already evidenced for magnetic removal of organic contaminants [7] and heavy metals in water treatment [8–13]. Nevertheless, in these works, authors use polymers or long chains to functionalize magnetite nanoparticles before application on metal removal.

To our knowledge, the papers that study the incorporation of amino acids in the elaboration of magnetic colloids deal normally with the synthesis of magnetite cores followed by its functionalization with different amino acids [14–19] or even synthesizing magnetite nanoparticles in the presence of amino acids, in one step [20]. Specifically for glycine, Viota et al. [21] discuss the electrokinetic characterization of magnetite nanoparticles functionalized with different amino acids, including glycine and Barick and Hassan [22] show a single-step approach for the synthesis of glycine-passivated Fe_3O_4 nanoparticles, both for biomedical applications. Thus, the innovation of this work is, mainly, the use of glycine-functionalized magnetic nanoparticles for the highly efficient magnetic removal of Cu^{2+} from wastewater. This indicates a cost-effective and environmentally friendly procedure since it involves a safe route of synthesis for magnetic nanograins and the use of the low-cost and low-toxicity molecules of glycine.

Inspite of the saturation magnetization of maghemite (γ-Fe_2O_3) being slightly lower than the one of magnetite (Fe_3O_4), maghemite was chosen in this work since the difference of magnetization is largely counterbalanced by the gain of chemical stability. In fact, magnetite nanoparticles can dissolve in acidic medium: this dissolution is faster as the particles size is smaller, and as the concentration of acid is higher [23]. In order to avoid this dissolution, magnetite can be deliberately oxidized to maghemite [24].

In the present work, a series of experiments of glycine adsorption on MNP from aqueous solutions at different initial concentrations and pHs were performed. To elucidate the interaction between glycine and maghemite during adsorption, several techniques, such as X-ray diffraction (XRD), transmission electron microscopy (TEM), magnetization measurements, dynamic light scattering (DLS), Fourier transform infrared (FTIR), and thermogravimetric analysis (TGA) were employed. Thus, the applicability of amine-functionalized NPs in the removal of Cu^{2+} was evaluated in the view of pH, time and adsorbate/adsorbent concentrations. The adsorption kinetics and adsorption isotherms were investigated by using the conventional models of adsorption. The synthesis method proposed here has some clear advantages including low-cost, simplicity, high quality, ease of scale-up and good reproducibility. Moreover, results indicate that copper adsorption capacity was larger than many other reports on the adsorption of metal ions by magnetic materials.

Table 1
Percentual of adsorbed glycine and surface coverage by ligand.

Mass ratio glycine:MNP		Surface coverage	
R_{GM} (%)	R'_{GM} (%)	(Molecules/nm^2)	θ
2	1.96	0.90	0.27
5	3.16	1.44	0.43
10	8.55	3.91	1.17
25	9.59	4.38	1.32
50	9.77	4.47	1.34
75	9.91	4.53	1.36

R_{GM} is the mass percentage of glycine used in functionalization, R'_{GM} is the mass percentage of glycine adsorbed on NPs and θ is the surface coverage in area by the molecules on the NPs.

2. Experimental

2.1. Synthesis of maghemite nanoparticles (MNP)

For the synthesis of γ-Fe_2O_3 nanoparticles, an adaptation of the method described in reference [25] was used: 50 mmol of NH_4OH was added to an aqueous solution containing 1.5 mmol of Fe^{2+} and 3.0 mmol of Fe^{3+} at room temperature. The resulting mixture was heated to reflux at boiling temperature under vigorous stirring. After 6 h precipitate was collected and washed with water several times after successive centrifugations.

2.2. Functionalization with glycine (Gly@MNP)

The typical approach employed for the functionalization of nanoparticles was used, as follows: 500 mg of MNP sample and an aliquot of 0.5 mol/L glycine, sufficient to give the mass ratios ($R_{G:M}$) between glycine and maghemite that are specified in Table 1, were introduced in a test tube. Thus, the pH was adjusted to the desired value and the volume completed to 2000 μL. After 60 min of mixing in a vortex agitator, solid was separated from supernatant by magnetic decantation or by centrifugation, washed once with water and dried under vacuum at room temperature.

2.3. Procedure of Cu^{2+} adsorption and kinetics

For adsorption investigation, in a typical experiment, 7.5 mg of the as-prepared Gly@MNP (R_{GM} = 10%) was added into a 50 mL of 5 mg/L Cu^{2+} solution. The mixture was adjusted to pH 6.5 with HCl and NaOH and stirred for 120 min. Thereafter, magnetic adsorbent with adsorbed copper ions were separated from the mixture with a permanent hand-held magnets (NdFeB ~ 0.3 T). The residual Cu^{2+} in the solution and nanoparticles was determined with ICP-OES [26]. In order to obtain the adsorption isotherms, solutions with varying initial concentration of copper were treated with the same procedure as above at room temperature. Control samples with only distilled water were utilized and monitored for the duration of all experiments.

2.4. Nanoparticles characterization

XRD was performed on powder samples with a Bruker D8-Focus Discover diffractometer using radiation of 1.541 Å (40 kV and 30 mA). TEM images were obtained on a JEOL 1100 microscope operating at an accelerating voltage of 80 kV. The room-temperature nanoparticle magnetization curves were obtained using an ADE vibrating sample magnetometer model EV7. Hysteresis loops were performed under applied magnetic fields varying from −18 to 18 kOe at 300 K. A dynamic light scattering analyzer

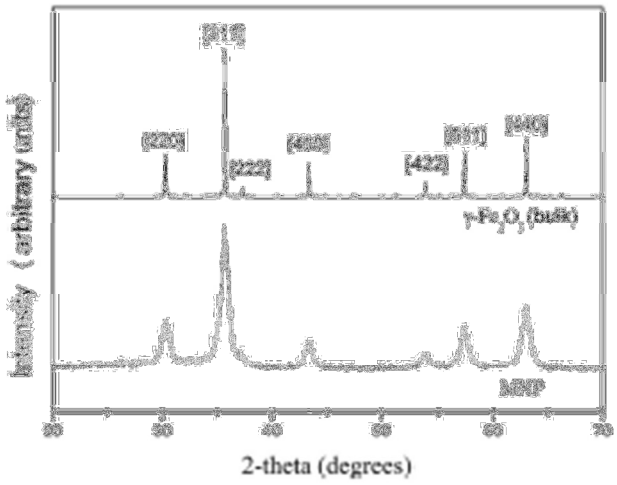

Fig. 1. XRD data of MNP sample and maghemite bulk standards (γ-Fe_2O_3).

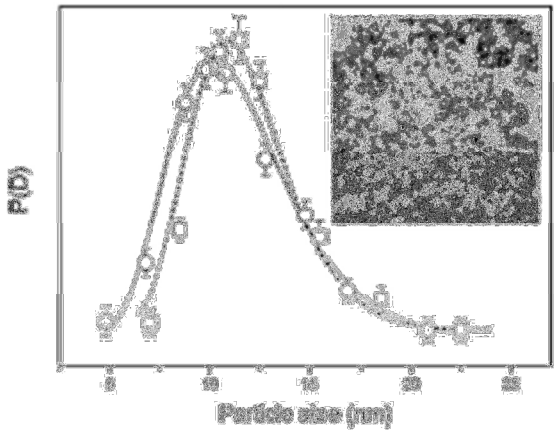

Fig. 2. Histograms from TEM measurements of MNP (circles) and functionalized (squares) samples. The full and dashed lines are the best fittings using log-normal distribution. The inset is a TEM image of MNPs (bar = 100 nm).

(Malvern Instrument, Zetasizer nano ZS) was used to measure the electrophoretic mobility. FTIR spectra were recorded with crystalline KBr in the range of 3700–400 cm^{-1} and resolution of 2 cm^{-1}. The deconvolution of the peaks was performed with the software Peakfit 4.12 using amplitude Gaussian model with linear baseline. TGA experiments were performed on a Shimadzu Thermogravimetric Analyzer model DTG-60, in dinitrogen flow and with a heating rate of 10 °C/min up to 550 °C, holding this temperature for 120 min.

3. Results and discussion

3.1. Synthesis of glycine-functionalized nanoparticles

The X-ray powder diffractograms of non-functionalized MNP and maghemite bulk standard are shown in Fig. 1. After indexing the main peaks using Bragg's law and comparing them to the ASTM data, spinel structure was found. Moreover, the experimental interplanar spacing of 0.834 nm compares well the ASTM *d*-spacing for cubic γ-Fe_2O_3 of 0.8347 nm, indicating that maghemite is the predominant crystalline phase in this sample. Additionally, the mean crystalline size of MNP was calculated from the most intense diffraction peak, resulting in a particle diameter 10.5 nm.

TEM measurements showed that synthesis yields nearly spherical NPs (see the inset of Fig. 2). Moreover, there is no significant difference between size distributions of functionalized nanoparticles and non-functionalized ones, as showed in Fig. 2.

Magnetization measurements were performed for evaluating the counterparts of functionalization in the magnetic properties of the NPs. Fig. 3(a) shows the room temperature magnetization curves for maghemite NPs and for one representative functionalized sample, which has about 10% in mass of glycine adsorbed. As expected for this size range, nanoparticles displayed features of superparamagnetism, such as negligible remanence and coercivity observed in hysteresis loops (see Fig. 3(b), which shows the magnetization data at low field range). It is interesting to mention that superparamagnetic properties are highly useful in the development of novel separation processes – that make nanograins prone to magnetic fields and they do not become permanently magnetized without an external magnetic field to support them. Moreover, there is no significant difference between saturation magnetization values of 47.4 emu/g and 45.9 emu/g for non-functionalized and functionalized samples respectively. Furthermore, if one normalizes magnetization only by the mass of the magnetic core (not the glycine), saturation magnetization of Gly@MNP sample is 47.8 emu/g. Besides, all these magnetizations are different from the bulk values for maghemite (60–80 emu/g), probably due to cationic redistribution [27] and surface and size-finite effects [28–30] that affect the magnetization characteristics of nanosized grains.

Thus, a series of experiments was performed to verify the best pH conditions for the functionalization of the MNPs by organic molecules. In this way, glycine at the mass ratio R_{GM} = 10% (glycine/MNP), was added to the suspensions containing oxide nanograins. Then, pH of solutions was adjusted to the desired value using diluted NaOH or HCl and, after centrifugation, the percentage of amino acid loaded by the MNPs was estimated by TGA. The column graph at the bottom of Fig. 4, which is a plot of the relative amount of adsorbed glycine at different pHs, shows that glycine is best adsorbed in the region of pH around 6. As pH

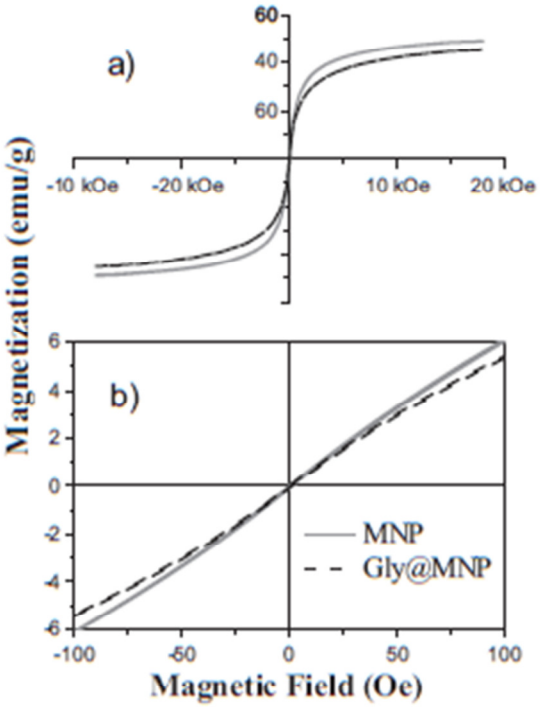

Fig. 3. (a) Magnetization curves of MNP and Gly@MNP samples. (b) Magnetization data at low field range.

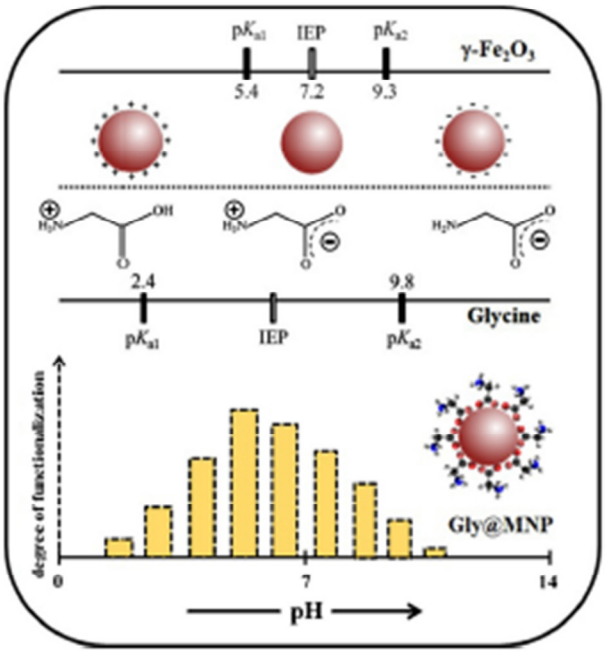

Fig. 4. Glycine adsorbate speciation and maghemite surface charge dependence on pH. The relative degrees of glycine adsorption (in arbitrary units) are plotted as a function of the pH at the bottom of figure for Gly@MNP.

increases or decreases from this value, the efficacy of functionalization decreases. To interpret these results, we took into account the fact that chemical states of the glycine molecule and MNPs surface are both strongly pH-dependent, as illustrated in the speciation schemes in Fig. 4.

As schematized, for MNPs, at low (high) pH values, the particles are positively (negatively) charged [31]. One can consider that superficial particle sites (▶) can undergo hydrolysis according to the acid–base reactions (1a) and (1b).

$$\blacktriangleright\!-OH_2^+ + H_2O \rightleftharpoons \blacktriangleright\!-OH + H_3O^+ \quad (1a)$$

$$\blacktriangleright\!-OH + H_2O \rightleftharpoons \blacktriangleright\!-O^- + H_3O^+ \quad (1b)$$

In this model, the particle surface behaves as a diprotic acid, leading to three kinds of surface sites where most of them are ▶—OH_2^+ in strong acidic medium, ▶—O^- in strong basic medium and ▶—OH, the intermediate amphoteric sites, in the isoelectric point (IEP) region. Quantitatively, when $pH = pK_{a1}$, ▶—OH_2^+ and ▶—OH are equimolar and if $pH = pK_{a2}$, [▶—OH] is equals [▶—O^-]. At IEP, ▶—OH is the predominant species.

According to reactions (2a) and (2b), for glycine, at very low pH, the predominant ionic species is the fully protonated form, ^+H_3N—CH_2—COOH. When $pH = pK_{a1}$, equimolar concentrations of ^+H_3N—CH_2—COOH and ^+H_3N—CH_2—COO^- species are present. At the IEP, glycine is present largely as the dipolar ion ^+H_3N—CH_2—COO^-. If $pH = pK_{a2}$, [^+H_3N—CH_2—COO^-] = [H_2N—CH_2—COO^-] and at high pH values, H_2N—CH_2—COO^- species predominates.

$$^+H_3N\text{–}CH_2\text{–}COOH + H_2O \rightleftharpoons {}^+H_3N\text{–}CH_2\text{–}COO^- + H_3O^+ \quad (2a)$$

$$^+H_3N\text{–}CH_2\text{–}COO^- + H_2O \rightleftharpoons H_2N\text{–}CH_2\text{–}COO^- + H_3O^+ \quad (2b)$$

The values of pK_{a1}, for reactions (1a) and (1b) and pK_{a2}, for reactions (2a) and (2b) as well as the values of IEP, are given in the scheme of Fig. 4. Thus, at low pH values, the glycinium cation is in contact with an increasingly positively charged oxide surface, so

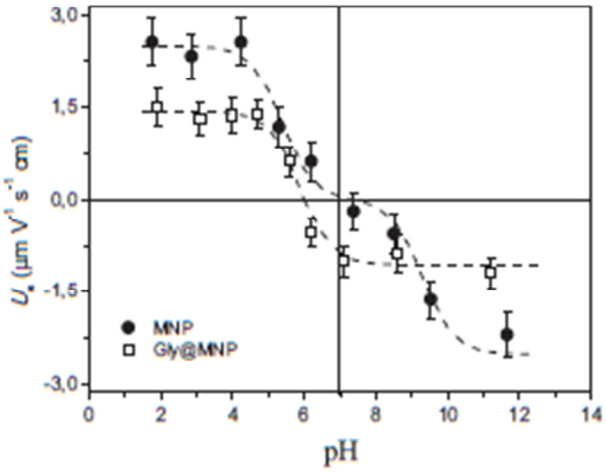

Fig. 5. Electrophoretic mobility (U_e) of MNP (circles) and Gly@MNP (squares) slurries as a function of pH. Dashed lines are guides for the eyes using the models of surface charge that are described in the text.

that electrostatic repulsion conduces to a low ligand adsorption. Besides, in high alkaline medium, the surface is strongly negative while the glycine speciation should favor the glycinate anion and, once more, electrostatic repulsions interfere in ligand adsorption. On the other hand, at pH around 6, a significant number of NPs are positively charged and glycine is quantitatively in the zwitterionic form. Thus, approximation of glycine to the metallic sites of surface is more favorable, and interaction of ▶—OH_2^+ with carboxylate could occur as schematized by the reaction (3).

$$\blacktriangleright\!-OH_2^+ + {}^+H_3N\text{–}CH_2\text{–}COO^- \longrightarrow \blacktriangleright\!-OOC\text{–}CH_2\text{–}NH_3^+ + H_2O \quad (3)$$

Moreover, functionalized particle surface can be seen as a monoprotic weak acid that undergoes hydrolysis according to the schematic acid–base reaction (4).

$$\blacktriangleright\!-OOC\text{–}CH_2\text{–}NH_3^+ + H_2O \rightleftharpoons \blacktriangleright\!-OOC\text{–}CH_2\text{–}NH_2 + H_3O^+ \quad (4)$$

The dependence of the electrophoretic mobility (U_e), obtained from DLS measurements, on the pH of the slurry is presented in Fig. 5. For bare MNPs the dependence of the surface charge on the pH is already well known and shows that for extreme pH values, surface charge reaches the maximum and close to pH = 7, the surface charge is very small as observed in Fig. 5. Using a model that describes particle surface as a diprotic weak acid [31], one plots a particle-charge curve which guides experimental points and permits the IEP of MNP to be estimated at pH ~ 7.3. For Gly@MNP, the surface is positively saturated in strong acidic media ($U_e \sim +15\,m\,s^{-1}\,V^{-1}\,cm$), but, as pH decreases, surface discharging takes place and the net charge becomes negligible at pH ~ 5.9. Thus, the fact that IEP of bare MNPs shifts about two pH units when particles are functionalized is in favor of the adsorption of organic molecules by MNPs. Here, the functionalized surface is considered to be a monoprotic acid (see reaction (4)) to generate the curve that guides the experimental points. According to this model, as pH increases from acid to IEP, the fraction of protonated ▶—OOC—CH_2—NH_3^+ group diminishes and that of ▶—OOC—CH_2—NH_2 increases. As the pH of slurry increases over PZN, NPs become negatively charged, saturating at $U_e = -11\,\mu m\,s^{-1}\,V^{-1}\,cm$. This could be due to the formation of the negatively charged species (▶—OOC—CH_2—NH_2OH^-) or by the fact that, in these conditions, glycine is partially desorbed from the surface and thus net charge of Gly@MNP – in neutral and more alkaline media – could be a balance between the charges of amine groups of adsorbed molecules and the charges of non-coordinated superficial sites.

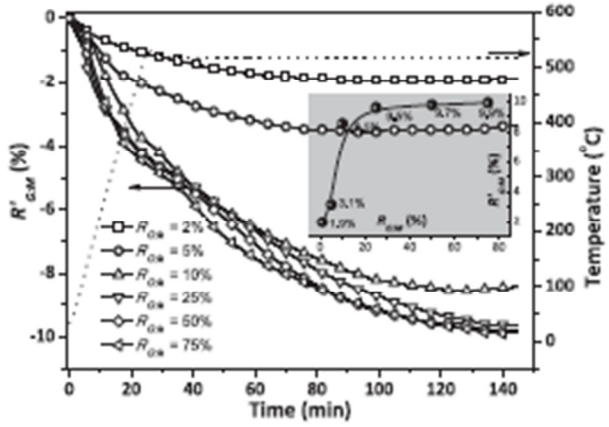

Fig. 6. TGA curves of weight loss versus time for functionalized NPs. Dashed curve represents the heating profile and the inset displays the amount of adsorbed glycine ($R'_{G:M}$) as a function of glycine concentration used in functionalization ($R_{G:M}$).

The experiments about the dependence of glycine adsorption on the ligand concentration were performed at pH = 6, using the Gly/MNP mass ratios ($R_{G:M}$) that are listed in Table 1.

For an accurate quantification, the amounts of adsorbed glycine were determined by thermogravimetry as described before [32]. Here, most of the loss in mass presented by the functionalized samples is attributed to the thermal decomposition of the adsorbed glycine, with a first region of loss of mass that occurs at lower temperatures due to the release of water. In this way, Fig. 6 shows the TGA curves – weight loss percentage (right axis) versus time – for samples prepared with different concentrations of glycine. In the curves of samples prepared with different concentrations of glycine one observes that the weight loss percentage increases until 120 min and thereafter remains practically constant for all studied samples. The mass percentages of adsorbed glycine on MNPs ($R'_{G:M}$), quantified from these curves, are listed in Table 1 and plotted as a function of $R_{G:M}$ in the graph of the inset in Fig. 6. It was found that increasing amounts of glycine are adsorbed as the concentration of glycine used in functionalization rises. Nevertheless, saturation of coating is achieved with the equilibrium of glycine concentration at $R_{G:M} \sim 10\%$.

Using the specific surface area of 175 m^2/g obtained from BET analysis, the number of glycine molecules per nm^2 estimated. Moreover, if one considers the cross-sectional area of one molecule of glycine to be ~0.3 nm^2 [33], the surface coverage (θ) can be estimated in terms of glycine monolayers using the quotient between the total area of ligand and MNP surface. The θ values displayed in Table 1 indicate that the NPs are covered by at least one monolayer of glycine when saturated with ligands. The adsorption isotherms at room temperature do not correspond to Langmuir type behavior. In fact the plot of the inverse of the concentration of adsorbed glycine versus the equilibrium concentration is strongly nonlinear. Also, other adsorption models were not able to fit our experimental results and calculate maximum adsorption parameters. This deviation could be associated to a possible rough inhomogeneous adsorbate surface with multiple site-types available for adsorption and to a possible adsorbate/adsorbate interaction. Results of FTIR and SAXS (see supplementary data) are in favor of this last observation. Thus, all the characterizations and adsorption experiments were performed using $R_{G:M} = 10\%$, in which the nanoparticles are supposed to be saturated of glycine molecules.

Fig. 7 shows the FTIR spectra of pure glycine (Gly), bare MNPs and Gly@MNP and their correspondent assignments. Fig. 7(c) also shows the Gaussian band deconvolution procedure corresponding to the envelopes of amine moiety bending mode ($\delta(NH_3)$) and

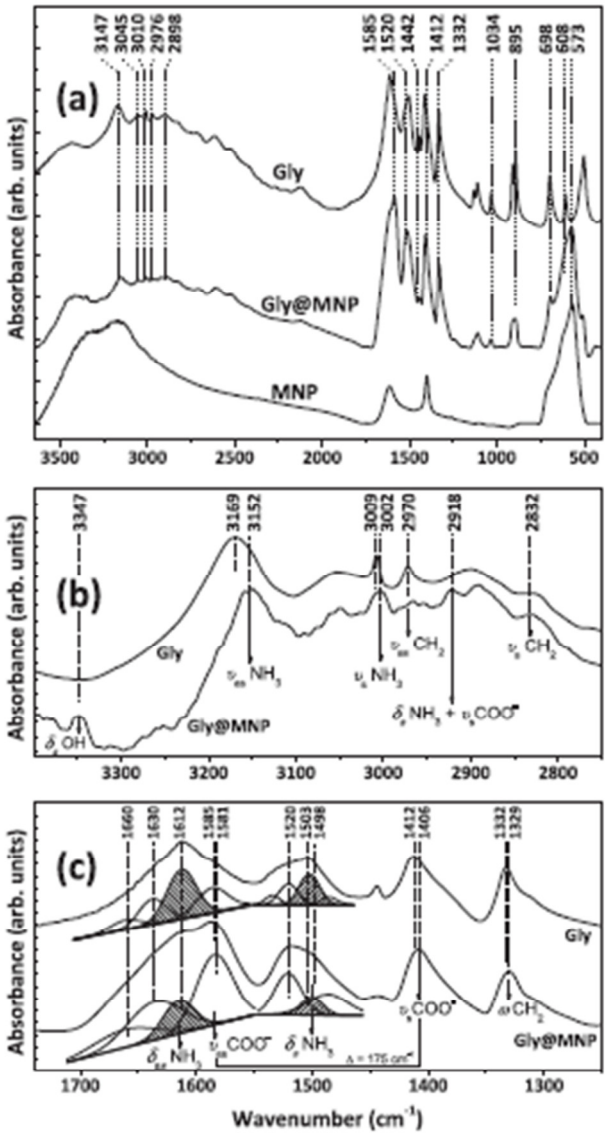

Fig. 7. (a) and (b) FTIR spectra of pure glycine, bare MNP and Gly@MNP and their correspondent assignments. (c) Gaussian band deconvolution procedure corresponding to the $\delta(NH_3)$ and $\nu(COO^-)$ envelope.

the carboxylate stretching modes ($\nu(COO^-)$). In Fig. 7(a) the IR bands verified around 573 cm^{-1} are commonly attributed to ferrite Fe—O absorptions [34,35], as well the contribution of the absorption at 3347 cm^{-1} displayed in Fig. 7(b), which is related to $\nu_s(OH)$ from oxide surface [36–38]. Simultaneously, most of the vibrational modes that correspond to pure glycine are also verified in the spectra of glycine coated samples [39,40]. Moreover, the wavenumber separation ($\Delta = 175\ cm^{-1}$) between asymmetric, $\nu_{as}(COO^-)$, and symmetric, $\nu_s(COO^-)$, stretching modes indicates a bridging bidentate interaction type of COO^- group with nanoparticle surface in good agreement with reference [41].

It is interesting to note that all vibrational modes related to the stretching and deformation absorption bands of COO^- and NH_3 groups from glycine, found in 1414, 1503, 1585, 3009 and 3169 cm^{-1}, are shifted about 5 cm^{-1} to lower wavenumbers upon the coating process, as verified in Fig. 7(b) and (c), and as described before [22]. Furthermore it seems that the $\nu_s(NH_3)$ is extensively involved in Fermi resonance with combination bands. In fact, in

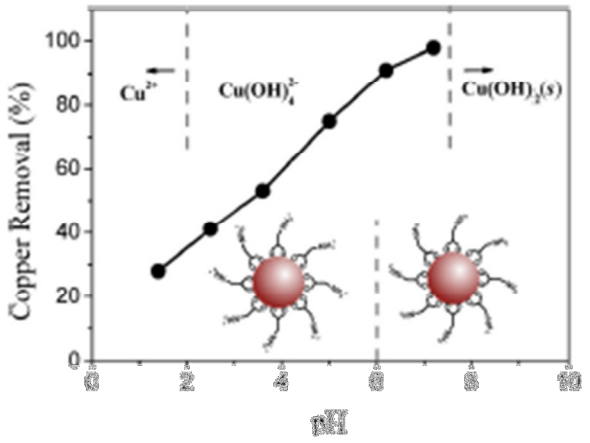

Fig. 8. Copper removal efficiency at different pH at 25 °C, using 7.5 mg of adsorbent, 50 mL of 10 mg/L of Cu^{2+} and a contact time of 1 h.

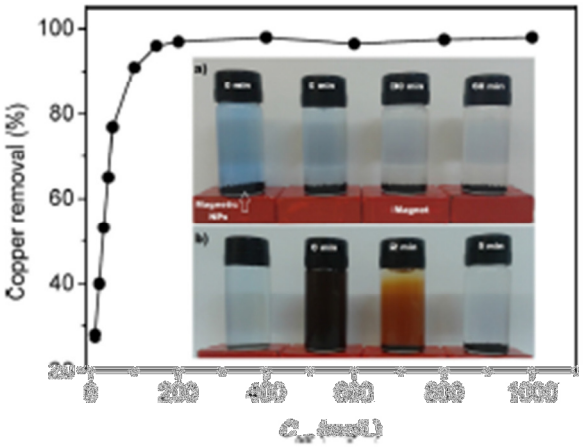

Fig. 9. Copper removal efficiency as a function of the concentration of Gly@MNP, at pH = 6.5, 25° C, in 50 mL of 10 mg/L of Cu^{2+} and a contact time of 1 h. Inset: (a) decrease of copper concentration (evidenced by the blue color) after treatment with magnetic nanoparticles using different times and (b) the efficiency of magnetic collectability of nanoparticles.

the spectrum for nanoparticles coated with glycine, the band at 2918 cm^{-1} in Fig. 7(b), resulting mainly from Fermi interaction with $\delta_s(NH_3)$ and $\nu_s(COO^-)$ (1500+1410 cm^{-1}), has been already attributed to zwitterionic and acid salt glycine forms [42]. Although still controversial, an interaction is suggested between $\delta_s(NH_3)$ and $\nu_s(COO^-)$ groups [43], indicating no less than two glycine coatings on analyzed nanoparticles. This interpretation is reinforced by the fact that in the spectra of nanoparticle coated with glycine verified in Fig. 7(c), the area of the symmetric and asymmetric deformation for NH_3 group observed in 1612 and 1503 cm^{-1} [43] corresponds to 15.4 and 17.6%, respectively, of total area of the absorption of this envelope. In the spectrum for pure glycine in Fig. 7(c) the percentages of these same areas are 44.5 and 50.7%, reaching the same proportion found in the coated sample. This decreasing intensity, in NH_3 deformation bands for functionalized samples, suggests a molecular interaction of this group with COO^- group.

3.2. Investigation of the Cu^{2+} removal

Initially, the influence of pH on the removal of Cu^{2+} from aqueous solution was investigated. In this way, a fixed quantity of Gly@MNP was mixed in a Cu^{2+} solution and the pH was adjusted. As observed in Fig. 8, adsorption of copper increases as pH increases from 1 up to 7. This behavior can be understood taking into account the speciation of copper and Gly@MNP nanoparticles as schematized in Fig. 8. At the range of concentration studied here, Cu^{2+} species only exists as free ions at very low pH and form soluble complexes with water at pH > 2 through the chemical reaction $Cu^{2+} + 4OH^- \rightarrow [Cu(OH)_4]^{2-}$ – with an equilibrium constant of 3×10^6. As the concentration of OH^- increases, a blue precipitate takes place – $Cu^{2+} + 2OH^- \rightarrow Cu(OH)_2$, $K_{ps} \sim 5 \times 10^{-20}$. Investigation of copper removal in alkaline media was not performed since when pH > 7, Cu^{2+} precipitates. Assuming that the concentration of ionic species must be sufficiently high as to overlap the electric double layers of the coated-nanoparticles, it seems that complexation and electrostatic forces have to be the responsible for the copper adsorption on functionalized nanoparticles [44]. At very low pH, copper ions and NPs are positively charged and electrostatic repulsions interfere in copper adsorption. As pH increases, the electrostatic attraction between the negative charged copper complex and positively charged NPs is in favor of adsorption. Maximal adsorption occurs at pH around 6.5, where the electrostatic interaction between residual protonated amine and copper aquocomplexes (▶ $-OOC-CH_2-NH_3^+ \cdots [Cu(OH)_4]^{2-}$) and/or surface complexation with non-protonated amine groups and copper (▶ $-OOC-CH_2-NH_2 \cdots Cu^{2+}$) may occur.

Fig. 9 shows the Cu^{2+} removal efficiency in flasks containing Cu^{2+} and different concentrations of Gly@MNP (C_{NP}). Adsorption of copper increased with the increase of adsorbent concentration and reached to plateau at $C_{NP} \sim 150$ mg/L. The inset (a) of Fig. 9 shows pictures of copper solution after treatment with nanoparticles using different times and (b) the collectability efficiency. Ammonium hydroxide was utilized to reveal the presence of Cu^{2+} in both solution, since it forms a blue soluble complex $[Cu(NH_3)_4]^{2+}$.

Cooper is quickly adsorbed by Gly@MNP during the first 25 min, thus adsorption reached the equilibrium as shown in Fig. 10, which is a plot of the variation of the metal concentration (C_t/C_0) in aqueous phase as a function of the time of contact with adsorbent. C_t and C_0 corresponds, respectively, to the copper concentration at time t and to the initial Cu^{2+} concentration. In order to evaluate the kinetic mechanism which controls the process of copper adsorption on functionalized nanoparticles, several models were utilized for analyzing the adsorption kinetics data and best results were obtained using the pseudo second-order model [45]. In this model, the linear form can be written as $t/q_t = (1/kq_e^2) + (1/q_t)$, where k is

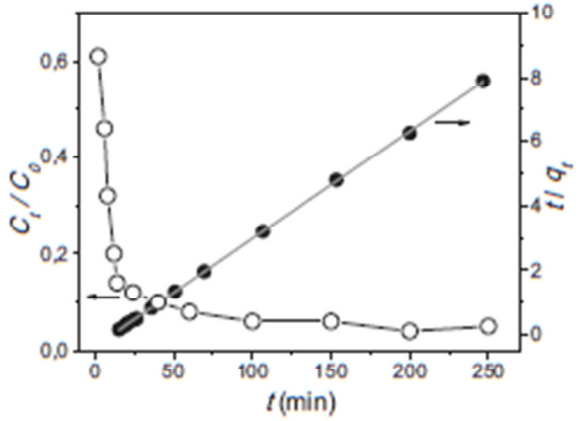

Fig. 10. Application of kinectic pseudo second-order linear model (gray line) to the experimental data (full circles). The open circles show the variation of copper concentration as a function of the time, using 7.5 mg of adsorbent and 50 mL of copper solution at pH = 6.5 and 25° C.

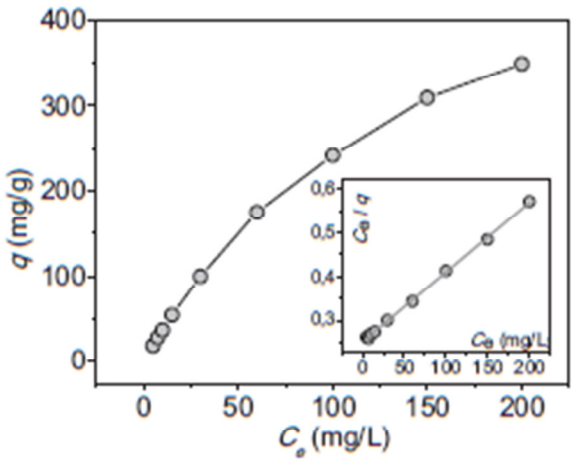

Fig. 11. Equilibrium isotherm for Cu^{2+} adsorption by glycine-modified maghemite nanoparticles at 25 °C and pH = 6.5. The inset shows the Langmuir adsorption isotherm fit of Cu^{2+} adsorption.

the pseudo second-order equilibrium constant and q_e and q_t are the adsorbed amount of solute at equilibrium and time t, respectively.

In this way, the linear fitting of experimental data on the graph of Fig. 10 (right axis) – a plot of t/q_t versus t – provided an excellent linearity ($R^2 > 0.999$). From the intercept of the straight line and slope of the graph, the values of $q_e = 32.1$ mg/g and $k = 8.0 \times 10^{-5}$ mg g^{-1} min^{-1}. The calculated value of q_e agrees with the adsorbed amount of Cu^{2+} at equilibrium determined experimentally. These results indicate that adsorption rate is a function of the concentration of free and adsorbed copper ions and coordination and electrostatic attractions between copper and functionalized surface are the main driving forces for the adsorption [45].

To investigate the details about adsorption, equilibrium studies were carried out at pH = 6.5 and time conditions needed to reach the adsorption equilibrium. In this way, the adsorption was measured using a fixed quantity of Gly@MNP and a varied copper concentration in solution. After cooper dosage, the isotherm – the concentration of adsorbed copper (q) at equilibrium as a function of the equilibrium concentration of free Cu^{2+} (C_e) – in Fig. 11 was plotted. Results show a non-linear increasing adsorption of copper as the concentration of free ions increases. Based on the assumptions that adsorption occurs in a monolayer on homogeneous particle surface with identical sites in terms of energy and negligible interaction among adsorbed species, the Langmuir adsorption model [45] was utilized to fit the experimental data. In this way, the linear form of the Langmuir equation $C_e/q = (1/k_L q_m) + (C_e/q_m)$ was employed.

The graph of C_e/q versus C_e shown on the inset of Fig. 11 allows the calculation of the maximum quantity of adsorption, q_m and the adsorption equilibrium constant, k_L. The linear fit of the data provided a $R^2 = 0.999$, $q_m = 625$ mg/g and $k_L = 6.5 \times 10^{-3}$. The value of maximum adsorption capacity (625 mg/g) found in this work is higher than many reported results also using amino-functionalized magnetic nanosystems (~27 mg/g [46], ~30 mg/g [13], ~46 mg/g [47] and ~524 mg/g [10]). This can be associated to the small size and large surface of particles and, high-affinity of nanograins for copper ions. In fact, it is well known that $-NH_2$ groups present at nanograins surface have a high binding affinity for organic matter [7] and for several metal ions, including Cu^{2+} investigated here. Thus, competitive adsorption of other contaminants as (Cr^{3+}, Co^{2+}, Ni^{2+}, Cd^{2+}, Pb^{2+} and As^{3+}) and even bacterial pathogens could be performed with our nanomaterials as reported before, using amino-functionalized magnetic nanograins [48].

Moreover, the large ratio saturation magnetization/particle size allows a quick and efficient magnetic separation and recovery of adsorbent phase. In fact, copper ions can be desorbed from magnetic nanoparticles by HCl solution (see supplementary data). After four cycles, the copper removal efficiency is still 89%, value comparable to previous work [13], suggesting that our Gly@MNP has good adsorption capability and desorption property to be recycled for copper adsorption.

4. Conclusions

Using an aqueous method of co-precipitation 12 nm sized maghemite nanoparticles were synthesized. Besides, it was observed that glycine is best adsorbed at pH ~ 6 and that saturation of oxide surface occurs with at least one monolayer of ligand, when glycine concentration reaches about 10% (w/w) on functionalized nanoparticles. Specifically, the carboxylate groups of glycine strongly coordinate to iron cations on the maghemite surface to form a robust coating, while the functionalized exteriors (amino groups) remained in the water medium. It has been observed that these glycine-modified NPs have strong affinity for the Cu^{2+}, probably due to electrostatic attraction and complexation of copper with NPs surface. The adsorption kinetics, highly dependent on the pH of the medium, followed a pseudo second-order mechanism. The adsorption equilibrium followed a Langmuir isotherm, giving a very high maximum capacity of copper adsorption. More specifically, our results suggest that these surface engineered magnetic nanoparticles are highly effective, efficient and economically viable magnetic nanoadsorbents for the removal of copper – and can be extended to other metals since amine groups present high binding affinity for metal complexation – from water in comparison to the existing industrial purification processes. Furthermore, these magnetic nanoadsorbents may be separated easily from the solution with the help of an external magnetic force and are reusable after removing the adsorbed toxic contaminants.

Acknowledgments

The authors thank Conselho Nacional de Desenvolvimento Científico e Tecnológico (CNPq) and Fundacão de Apoio à Pesquisa do Distrito Federal (FAPDF) for financial support. MHS and JCR thank CNPq for a research fellowship. Authors also thank the National Synchrotron Light Laboratory (LNLS – proposal 14384).

Appendix A. Supplementary data

Supplementary data associated with this article can be found, in the online version, at http://dx.doi.org/10.1016/j.jhazmat.2013.11.022.

References

[1] M. Hua, S.J. Zhang, B.C. Pan, W.M. Zhang, L. Lv, Q.X. Zhang, Heavy metal removal from water/wastewater by nanosized metal oxides: a review, J. Hazard. Mater. 211 (2012) 317–331.
[2] J. Schulte, J. Dutta, Nanotechnology in environmental protection and pollution, Sci. Technol. Adv. Mater. 6 (2005) 219–220.
[3] A.F. Ngomsik, A. Bee, M. Draye, G. Cote, V. Cabuil, Magnetic nano- and microparticles for metal removal and environmental applications: a review, R. Chimie 8 (2005) 963–970.
[4] L. Carlos, F.S. García Einschlag, M.C. González, D.O. Mártire, Applications of magnetite nanoparticles for heavy metal removal from wastewater, in: F.S. García Einschlag, L. Carlos (Eds.), Waste Water – Treatment Technologies and Recent Analytical Developments, InTech, Rijeka, 2013, pp. 63–78.
[5] A. Bée, D. Talbot, S. Abramson, V. Dupuis, Magnetic alginate beads for Pb(II) ions removal from wastewater, J. Colloid Interface Sci. 362 (2011) 486–492.

[6] M. Auffan, H.J. Shipley, S. Yean, A.T. Kan, M. Tomson, J. Rose, J.Y. Bottero, Nanomaterials as adsobents, in: M.R. Wiesner, J.Y. Bottero (Eds.), Environmental Nanotechnology: Applications and Impacts of Nanomaterials, McGraw-Hill, New York, 2007, pp. 371–392.
[7] C.C.P. Chan, H. Gallard, P. Majewski, Fabrication of amine-functionalized magnetite nanoparticles for water treatment processes, J. Nanopart. Res. 14 (2012).
[8] X. Xin, Q. Wei, J. Yang, L. Yan, R. Feng, G. Chen, B. Du, H. Li, Highly efficient removal of heavy metal ions by amine-functionalized mesoporous Fe_3O_4 nanoparticles, Chem. Eng. J. 184 (2012) 132–140.
[9] Y.F. Lin, H.W. Chen, K.L. Lin, B. Chen, C. Chiou, Application of magnetic particles modified with amino groups to adsorb copper ions in aqueous solution, J. Environ. Sci. – China 23 (2011) 44–50.
[10] I.Y. Goon, C.C. Zhang, M. Lim, J.J. Gooding, R. Amal, Controlled fabrication of polyethylenimine-functionalized magnetic nanoparticles for the sequestration and quantification of free Cu^{2+}, Langmuir 26 (2010) 12247–12252.
[11] S.H. Huang, D.H. Chen, Rapid removal of heavy metal cations and anions from aqueous solutions by an amino-functionalized magnetic nano-adsorbent, J. Hazard. Mater. 163 (2009) 174–179.
[12] C.M. Chou, H.L. Lien, Dendrimer-conjugated magnetic nanoparticles for removal of zinc (II) from aqueous solutions, J. Nanopart. Res. 13 (2011) 2099–2107.
[13] J.H. Wang, S.R. Zheng, Y. Shao, J.L. Liu, Z.Y. Xu, D.Q. Zhu, Amino-functionalized $Fe_3O_4@SiO_2$ core-shell magnetic nanomaterial as a novel adsorbent for aqueous heavy metals removal, J. Colloid Interface Sci. 349 (2010) 293–299.
[14] M.H. Sousa, J.C. Rubim, P.G. Sobrinho, F.A. Tourinho, Biocompatible magnetic fluid precursors based on aspartic and glutamic acid modified maghemite nanostructures, J. Magn. Magn. Mater. 225 (2001) 67–72.
[15] S.L. Tie, Y.Q. Lin, H.C. Lee, Y.S. Bae, C.H. Lee, Amino acid-coated nano-sized magnetite particles prepared by two-step transformation, Colloid Surf. A 273 (2006) 75–83.
[16] J.Y. Park, E.S. Choi, M.J. Baek, G.H. Lee, Colloidal stability of amino acid coated magnetite nanoparticles in physiological fluid, Mater. Lett. 63 (2009) 379–381.
[17] S. Ghosh, A.Z.M. Badruddoza, M.S. Uddin, K. Hidajat, Adsorption of chiral aromatic amino acids onto carboxymethyl-beta-cyclodextrin bonded Fe_3O_4/SiO_2 core-shell nanoparticles, J. Colloid Interface Sci. 354 (2011) 483–492.
[18] A. Ebrahiminezhad, S. Davaran, S. Rasoul-Amini, J. Barar, M. Moghadam, Y. Ghasemi, Synthesis, characterization and anti-*Listeria monocytogenes* effect of amino acid coated magnetite nanoparticles, Curr. Nanosci. 8 (2012) 868–874.
[19] R. Krishna, E. Titus, R. Krishna, N. Bardhan, D. Bahadur, J. Gracio, Wet-chemical green synthesis of L-lysine amino acid stabilized biocompatible iron-oxide magnetic nanoparticles, J. Nanosci. Nanotechnol. 12 (2012) 6645–6651.
[20] G. Marinescu, L. Patron, D.C. Culita, C. Neagoe, C.I. Lepadatu, I. Balint, L. Bessais, C.B. Cizmas, Synthesis of magnetite nanoparticles in the presence of aminoacids, J. Nanopart. Res. 8 (2006) 1045–1051.
[21] J.L. Viota, F.J. Arroyo, A.V. Delgado, J. Horno, Electrokinetic characterization of magnetite nanoparticles functionalized with amino acids, J. Colloid Interface Sci. 344 (2010) 144–149.
[22] K.C. Barick, P.A. Hassan, Glycine passivated Fe_3O_4 nanoparticles for thermal therapy, J. Colloid Interface Sci. 369 (2012) 96–102.
[23] J.P. Jolivet, E. Tronc, Crystallization of ferric hydroxide into spinel by adsorption on colloidal magnetite, J. Colloid Interface Sci. 150 (1992) 453–460.
[24] S. Lefebure, E. Dubois, V. Gabuil, S. Neveu, R. Massart, Monodisperse magnetic nanoparticles: preparation and dispersion in water and oils, J. Mater. Res. 13 (10) (1998) 2975–2981.
[25] A.L. Drummond, N.C. Feitoza, G.C. Duarte, M.J.A. Sales, L.P. Silva, J.A. Chaker, A.F. Bakuzis, M.H. Sousa, Reducing size-dispersion in one-pot aqueous synthesis of maghemite nanoparticles, J. Nanosci. Nanotechnol. 12 (2012) 8061–8066.
[26] M.H. Sousa, J.G. Silva, J. Depeyrot, F.A. Tourinho, L.F. Zara, Chemical analysis of size-tailored magnetic colloids using slurry nebulization in ICP-OES, Microchem. J. 97 (2011) 182–187.
[27] J.A. Gomes, M.H. Sousa, F.A. Tourinho, J. Mestnik, R. Itri, J. Depeyrot, Rietveld structure refinement of the cation distribution in ferrite fine particles studied by X-ray powder diffraction, J. Magn. Magn. Mater. 289 (2005) 184–187.
[28] E.C. Sousa, M.H. Sousa, G.F. Goya, H.R. Rechenberg, M.C.F.L. Lara, F.A. Tourinho, J. Depeyrot, Enhanced surface anisotropy evidenced by Mossbauer spectroscopy in nickel ferrite nanoparticles, J. Magn. Magn. Mater. 272 (2004) E1215–E1217.
[29] J.F. Saenger, K.S. Neto, P.C. Morais, M.H. Sousa, F.A. Tourinho, Investigation of the anisotropy in frozen nickel ferrite ionic magnetic fluid using magnetic resonance, J. Magn. Reson. 134 (1998) 180–183.
[30] C.R. Alves, R. Aquino, M.H. Sousa, H.R. Rechenberg, G.F. Goya, F.A. Tourinho, J. Depeyrot, Low temperature experimental investigation of finite-size and surface effects in $CuFe_2O_4$ nanoparticles of ferrofluids, J. Metastab. Nanocryst. 20/21 (2004) 694–699.
[31] F.A. Tourinho, A.F.C. Campos, R. Aquino, M.C.F.L. Lara, G.J. da Silva, J. Depeyrot, Surface charge density determination in electric double layered magnetic fluids, Braz. J. Phys. 32 (2002) 501–508.
[32] M. Meng, L. Stievano, J.F. Lambert, Adsorption and thermal condensation mechanisms of amino acids on oxide supports. 1. Glycine on silica, Langmuir 20 (2004) 914–923.
[33] J.W. Han, J.N. James, D.S. Sholl, Chemical speciation of adsorbed glycine on metal surfaces, J. Chem. Phys. 135 (2011) 034703 1–034703 8.
[34] C. Pereira, A.M. Pereira, C. Fernandes, M. Rocha, R. Mendes, M.P. Fernandez-Garcia, A. Guedes, P.B. Tavares, J.M. Greneche, J.P. Araujo, C. Freire, Superparamagnetic MFe_2O_4 (M = Fe, Co, Mn) nanoparticles: tuning the particle size and magnetic properties through a novel one-step coprecipitation route, Chem. Mater. 24 (2012) 1496–1504.
[35] L.V. Gasparov, D.B. Tanner, D.B. Romero, H. Berger, G. Margaritondo, L. Forro, Infrared and Raman studies of the Verwey transition in magnetite, Phys. Rev. B 62 (2000) 7939–7944.
[36] M.H. Sousa, F.A. Tourinho, J.C. Rubim, Use of Raman micro-spectroscopy in the characterization of $M(II)Fe_2O_4$ (M = Fe, Zn) electric double layer ferrofluids, J. Raman Spectrosc. 31 (2000) 185–191.
[37] G.V.M. Jacintho, A.G. Brolo, P. Corio, P.A.Z. Suarez, J.C. Rubim, Structural investigation of MFe_2O_4 (M = Fe, Co) magnetic fluids, J. Phys. Chem. C 113 (2009) 7684–7691.
[38] J.C. Rubim, M.H. Sousa, J.C.O. Silva, F.A. Tourinho, Raman spectroscopy as a powerful technique in the characterization of ferrofluids, Braz. J. Phys. 31 (2001) 402–408.
[39] M.L. Hair, Hydroxyl-groups on silica surface, J. Non-Cryst. Solids 19 (1975) 299–309.
[40] D. Predoi, E. Andronescu, M. Radu, M.C. Munteanu, A. Dinischiotu, Synthesis and characterization of biocompatible maghemite nanoparticles, Digest J. Nanomater. Biostruct. 5 (2010) 779–786.
[41] K. Nakamoto, Infrared and Raman Spectra of Inorganic and Coordination Compounds, 1st ed., Wiley, New York, 1986.
[42] C. Destrade, C. Garrigou-Lagrange, M.T. Forel, Détermination du champ de force de valence de l'ion $H_3N + CH_2COO^-$. Son apport dans l'étude de la conformation, J. Mol. Struct. 10 (1971) 203–219.
[43] M.T. Rosado, M.L.T.S. Duarte, R. Fausto, Vibrational spectra of acid and alkaline glycine salts, Vib. Spectrosc. 16 (1998) 35–54.
[44] J. Porath, B. Olin, Immobilized metal affinity adsorption and immobilized metal affinity chromatography of biomaterials. Serum protein affinities for gel-immobilized iron and nickel ions, Biochemistry 22 (1983) 1621–1630.
[45] D.D. Cooney, Adsorption Design for Wastewater Treatment, 1st ed., CRC Press, Boca Raton, 1998.
[46] C. Wilaiwan, S. Yongsoon, D. Joseph, D.S. William, H.L. Nikki, D.R. Ryan, E.F. Glen, S. Thanapon, Y. Wassana, Selective removal of copper(II) from natural waters by nanoporous sorbents functionalized with chelating diamines, Environ. Sci. Technol. 44 (2010) 6390–6396.
[47] J.F. Liu, Z.S. Zhao, G.B. Jiang, Coating Fe_3O_4 magnetic nanoparticles with humic acid for high efficient removal of heavy metals in water, Environ. Sci. Technol. 42 (2008) 6949–6954.
[48] S. Singh, K.C. Barick, D. Bahadur, Surface engineered magnetic nanoparticles for removal of toxic metal ions and bacterial pathogens, J. Hazard. Mater. 192 (2011) 1539–1547.

ANEXO E

Classificação Qualis da Capes para o periódico

Journal of Hazardous Materials

Consulta por Título

ISSN	TÍTULO	ESTRATO	ÁREA DE AVALIAÇÃO	STATUS
0304-3894	Journal of Hazardous Materials (Print)	A1	BIODIVERSIDADE	Atualizado
0304-3894	Journal of Hazardous Materials (Print)	A1	CIÊNCIA DE ALIMENTOS	Atualizado
0304-3894	Journal of Hazardous Materials (Print)	A1	CIÊNCIAS AGRÁRIAS I	Atualizado
0304-3894	Journal of Hazardous Materials (Print)	A1	CIÊNCIAS AMBIENTAIS	Atualizado
0304-3894	Journal of Hazardous Materials (Print)	A1	ENGENHARIAS I	Atualizado
0304-3894	Journal of Hazardous Materials (Print)	A1	ENGENHARIAS II	Atualizado
0304-3894	Journal of Hazardous Materials (Print)	A1	ENGENHARIAS III	Atualizado
0304-3894	Journal of Hazardous Materials (Print)	A1	FARMÁCIA	Atualizado
0304-3894	Journal of Hazardous Materials (Print)	A1	GEOCIÊNCIAS	Atualizado
0304-3894	Journal of Hazardous Materials (Print)	A1	GEOGRAFIA	Atualizado
0304-3894	Journal of Hazardous Materials (Print)	A1	INTERDISCIPLINAR	Atualizado
0304-3894	Journal of Hazardous Materials (Print)	A1	MATERIAIS	Atualizado
0304-3894	Journal of Hazardous Materials (Print)	A1	MEDICINA II	Atualizado
0304-3894	Journal of Hazardous Materials (Print)	A1	ODONTOLOGIA	Atualizado
0304-3894	Journal of Hazardous Materials (Print)	A1	QUÍMICA	Atualizado
0304-3894	Journal of Hazardous Materials (Print)	A2	BIOTECNOLOGIA	Atualizado
0304-3894	Journal of Hazardous Materials (Print)	A2	CIÊNCIAS BIOLÓGICAS I	Atualizado
0304-3894	Journal of Hazardous Materials (Print)	A2	CIÊNCIAS BIOLÓGICAS II	Atualizado
0304-3894	Journal of Hazardous Materials (Print)	A2	CIÊNCIAS BIOLÓGICAS III	Atualizado
0304-3894	Journal of Hazardous Materials (Print)	A2	ENGENHARIAS IV	Atualizado
0304-3894	Journal of Hazardous Materials (Print)	B1	ASTRONOMIA / FÍSICA	Atualizado
0304-3894	Journal of Hazardous Materials (Print)	B1	CIÊNCIA DA COMPUTAÇÃO	Atualizado
0304-3894	Journal of Hazardous Materials (Print)	B2	ENSINO	Atualizado